



**Sofia Isabel Esteves
Miguel**

**Medição e modelação de equilíbrios de fases
relevantes para a produção de biocombustíveis**

**Measurement and modelling of phase equilibria in
biofuel production**



**Sofia Isabel Esteves
Miguel**

**Medição e modelação de equilíbrios de fases na
produção de biocombustíveis**

**Measurement and modeling of phase equilibria in
biofuel production**

dissertação apresentada à Universidade de Aveiro para cumprimento dos requisitos necessários à obtenção do grau de Mestre em Engenharia Química, realizada sob a orientação científica do Professor Doutor. João A. P. Coutinho, Professor Associado com Agregação do Departamento de Química da Universidade de Aveiro e do Doutor. António José do Nascimento Queimada, Investigador Auxiliar do LSRE, Universidade do Porto.

Dedico este trabalho ao meu avô, aos meus pais e à minha irmã.

o júri

Presidente

Professor Doutor Dmitry Victorovich Evtugin

Professor associado com agregação do Departamento de Química da Universidade de Aveiro

Professor Doutor João Manuel da Costa e Araújo Pereira Coutinho

Professor associado com agregação do Departamento de Química da Universidade de Aveiro

Doutor António José Queimada

Investigador auxiliar da Faculdade de Engenharia da Universidade do Porto

Professor Doutor Nelson Simões Oliveira

Eq. professor adjunto do Instituto Politécnico de Leiria

agradecimentos

Antes de mais queria agradecer aos meus orientadores Prof. Dr. João A. P. Coutinho e Dr. António José Queimada pelo ensinamento e disponibilidade prestados durante a realização deste trabalho.

Ao grupo PATH, especialmente à Marianita, por toda a ajuda e apoio que me deu e por estar sempre disponível para qualquer coisa; à Maria Jorge e ao Pedro pela ajuda e instrução que me deram durante o tempo passado no laboratório.

À minha pequena grande amiga Ana Rute que esteve presente nos bons e nos maus momentos, e que estava sempre pronta para me apoiar e para me fazer rir mesmo quando eu achava que isso era impossível. Obrigada por tudo e por seres a pessoa excelente que és.

Aos meus amigos, principalmente à Joana, Carolina, Andreia, Paty, Inês, Ana, Vítor, João Tiago, Rúben, João Gonçalo, Gravilha, Clara, Beto e André pois estiveram sempre ao meu lado e sem eles nada era a mesma coisa.

À minha querida irmã pela paciência que teve e que tem para me aturar e porque sem ela não estaria aqui.

Aos meus pais e ao resto da minha família pela força que me deram e por terem acreditado que eu era capaz.

palavras-chave

Biocombustíveis, bioetanol, biodiesel, equilíbrio de fases, CPA EoS

resumo

O aumento do preço do petróleo e o seu consumo excessivo, o esgotamento das reservas de petróleo e as alterações climáticas resultantes da emissão de gases com efeito de estufa, tornaram necessário o desenvolvimento de combustíveis alternativos com base em fontes renováveis. Os biocombustíveis são uma alternativa aos combustíveis fósseis, sendo o biodiesel e o bioetanol os mais produzidos actualmente.

O bioetanol é produzido a partir de várias fontes renováveis, como a cana-de-açúcar, beterraba, milho, trigo ou madeira, que contêm elevadas percentagens de açúcares. Esses açúcares podem ser facilmente convertidos em etanol a partir da fermentação. Para separar o etanol da água, obtido na fermentação, várias técnicas podem ser utilizadas, como a destilação, adsorção, extracção líquido-líquido, entre outras. Neste trabalho foi estudado o equilíbrio de fases presente na extracção líquido-líquido.

Foram medidas tie-lines para dois sistemas líquido-líquido, óleo de rícino + água + etanol e laurato de metilo + água + etanol.

O biodiesel é produzido a partir de óleos vegetais e gorduras animais, a partir da reacção de transesterificação com álcoois de cadeia curta. Nesta reacção os óleos e gorduras reagem com o álcool na presença de um catalisador, para se obterem os correspondentes ésteres alquílicos.

O conhecimento do equilíbrio de fases dos sistemas que contêm álcoois e ésteres de ácidos gordos, é necessário para conceber e desenvolver os processos de purificação e produção do biodiesel. Foi medido o equilíbrio líquido-vapor (VLE) de sistemas de ésteres metílicos de ácidos gordos + álcoois, uma vez que os dados existentes na literatura relativamente a estes compostos são escassos.

A equação de estado CPA (Cubic-Plus-Association) foi aplicada com sucesso aos dados experimentais de equilíbrio líquido-vapor.

keywords

Biofuel, biodiesel, bioethanol, phase equilibria, CPA EoS

abstract

With the increase of the oil price and its excessive consumption, the depletion of oil resources and climate change derived from the emission of greenhouse gases, the development of alternative fuels based on renewable sources became necessary. Biofuels are an alternative for fossil fuels, being the most important today the biodiesel and bioethanol.

Bioethanol is produced from many renewable sources, such as sugar cane, sugar beet, corn, wheat and wood, which contain high percentages of sugars. These sugars can be easily converted to ethanol by fermentation. To recover the ethanol from fermentation broths, several techniques can be used, such as distillation, adsorption, liquid-liquid extraction, among others. In this work, the phase equilibria in liquid-liquid extraction was studied.

Liquid-liquid equilibria (LLE) tie-lines were measured for two systems, castor oil -water-ethanol and methyl laurate-water-ethanol.

Biodiesel is produced from vegetable oils and animals fats, through transesterification with lower alcohols. In this reaction vegetable oils and/or animal fats react with an alcohol in the presence of a catalyst, to give the corresponding alkyl esters.

The knowledge about the phase equilibria of systems containing an alcohol and a fatty acid ester is thus necessary to correctly design and develop biodiesel production and purification processes.

The vapor-liquid equilibria (VLE) for fatty acid methyl esters + alcohols systems was measured with an ebulliometer, as information about this kind of data was surprisingly scarce in the literature.

The CPA (Cubic-Plus-Association) Equation of State was successfully applied to model the new experimental VLE data.

Contents

List of tables	VIII
List of figures	IX
List of symbols	XI
Part I. Introduction.....	1
1. Biofuels	4
1.1 Bioethanol.....	6
1.1.1 Bioethanol production	6
1.1.2 Ethanol recovery	8
1.2 Biodiesel	10
1.2.1 Biodiesel production	10
1.2.2 Biodiesel production and purification process	12
2. Model	15
Part II. Experimental.....	21
1. Liquid-liquid equilibria	23
2. Vapor-liquid equilibria	25
Part III. Results and discussion	29
1. Liquid-liquid equilibria	31
2. Vapor-liquid equilibria	34
2.1 Experimental data	34
2.2 Modeling	39
Part IV. Conclusions	47
Part V. Bibliographic References	51
Appendix	59
A Calibration curves for ethanol + FAME systems	61
B Calibration curves for methanol + FAME systems	63

List of tables

Table 1 World primary energy demand (Mtoe) [2].....	4
Table 2 Biodiesel production input and output levels [28].....	12
Table 3 Association schemes [33, 47]	18
Table 4 Types of bonding in associating fluids [33, 47].	19
Table 5 Specifications of the chemicals	25
Table 6 Tie line data for castor oil(S) + ethanol(E) + water(W) system (weight fraction). 32	
Table 7 Tie line data for methyl laurate(S) + ethanol(E) + water(W) (weight fraction).....	33
Table 8 CPA Pure-compound parameters and modeling results	39
Table 9 CPA binary interaction parameters for ethanol + ester systems.....	40
Table 10 CPA binary interaction parameters for methanol + ester systems.....	41

List of figures

Figure 1 World primary energy demand by fuel [2].	3
Figure 2 Trend in world biofuel production [9].	5
Figure 3 Some raw materials for bioethanol and biodiesel [11].	6
Figure 4 World bioethanol production, trade and prices, with projections to 2017.[13]	8
Figure 5 Ternary diagram [22].	10
Figure 6 Transesterification reaction [26].	11
Figure 7 World biodiesel production, trade and prices, with projections to 2017 [13].	12
Figure 8 Diagram of biodiesel production process [29].	14
Figure 9 Biphasic sample.	23
Figure 10 Metrohm 831 Karl Fischer Coulometer.	24
Figure 11 Vacuum line.	24
Figure 12 Ebulliometer.	26
Figure 13 Abbe refractometer.	27
Figure 14 Ternary diagram of castor oil + ethanol + water system in weight fraction.	31
Figure 15 Ternary diagram of methyl laurate+ethanol+water system in weight fraction.	32
Figure 16 VLE for ethanol + methyl laurate system.	34
Figure 17 VLE for ethanol + methyl myristate system.	35
Figure 18 VLE for ethanol + methyl palmitate system.	35
Figure 19 VLE for ethanol + methyl oleate system.	36
Figure 20 VLE for methanol + methyl laurate system.	37
Figure 21 VLE for methanol + methyl myristate system.	37
Figure 22 VLE for methanol + methyl oleate system.	38
Figure 23 k_{ij} trend with the ester carbon number for ethanol + ester systems.	40
Figure 24 k_{ij} trend with the ester carbon number for methanol + ester systems	41
Figure 25 VLE for ethanol + methyl laurate system with $k_{ij}=-0,0002$.	42
Figure 26 VLE for ethanol + methyl myristate system with $k_{ij}=-0,0046$.	42
Figure 27 VLE for ethanol + methyl oleate system with $k_{ij}=-0,0197$.	43
Figure 28 VLE for methanol + methyl laurate system with $k_{ij}=-0,0326$.	44
Figure 29 VLE for methanol + methyl myristate system with $k_{ij}=-0,0432$.	45
Figure 30 VLE for methanol + methyl oleate system with $k_{ij}=-0,0589$.	45

Figure A 1 Calibration curve of ethanol + methyl laurate system.	61
Figure A 2 Calibration curve of ethanol + methyl myristate system.	61
Figure A 3 Calibration curve of ethanol + methyl palmitate system.	62
Figure A 4 Calibration curve of ethanol + methyl oleate system.	62
Figure B 1 Calibration curve of methanol + methyl laurate system.	63
Figure B 2 Calibration curve of methanol + methyl myristate system.....	63
Figure B 3 Calibration curve of methanol + methyl oleate system.....	64

List of symbols

a	energy parameter in the physical term
a_0	parameter in the energy term
A_i	site A in molecule i
b	co-volume
B_j	site B in molecule j
c_1	parameter in the energy term
g	simplified hard-sphere radial distribution function
K_{DE}	distribution coefficient for ethanol
K_{DW}	distribution coefficient for water
k_{ij}	binary interaction parameter
P	pressure
R	gas constant
T	temperature
T_c	critical temperature
V_m	molar volume
w	weight fraction
X_{Ai}	fraction of molecule i not bonded at site A
x_i	liquid mole fraction of component i
y_i	vapor mole fraction of component i
Z	compressibility factor

Greek Letters

α	separation factor
β	association volume parameter
Δ	association strength
ε	association energy
η	reduced fluid density
ρ	molar density

Subscripts

b	bubble
c	critical
i,j	pure component indexes
r	reduced

Superscripts

assoc.	association
calc	calculated value
exp	experimental value
phys.	physical

List of Abbreviations

AAD	average absolute deviation
ap	aqueous phase
CPA	cubic-plus-association
CR	combining rule
EoS	equation of state
FAME	fatty acid methyl ester
LLE	liquid-liquid equilibria
NP	number of points
OF	objective function
op	organic phase
SRK	Soave-Redlich-Kwong
toe	tonnes of oil equivalent
VLE	vapor-liquid equilibria

Part I. Introduction

Since the beginning of humanity, energy is the driving force of development, which became more pronounced from the Industrial Revolution onwards. Nowadays the energy is one of the most important factors in the development of countries.

Energy can be divided in two types, primary and secondary energy. Primary energy is the energy that exists in natural form and can generate energy in a direct way, such as oil, coal, natural gas, wind, water in dams, solar energy and geothermal energy. This can be classified into renewable and non-renewable energy. The secondary energy is obtained from the transformation of primary energy, such as electricity, gasoline, diesel, among others[1].

The demand of global primary energy is estimated to increase by 52% from 2003 to 2030, reaching 16.3 billion tonnes of oil equivalent (toe). Although fossil fuels are non renewable sources of energy, they will continue to be used as main sources of primary energy. The use of other renewable energy sources will increase progressively, but remains at low levels compared to the demand of oil [2, 3].

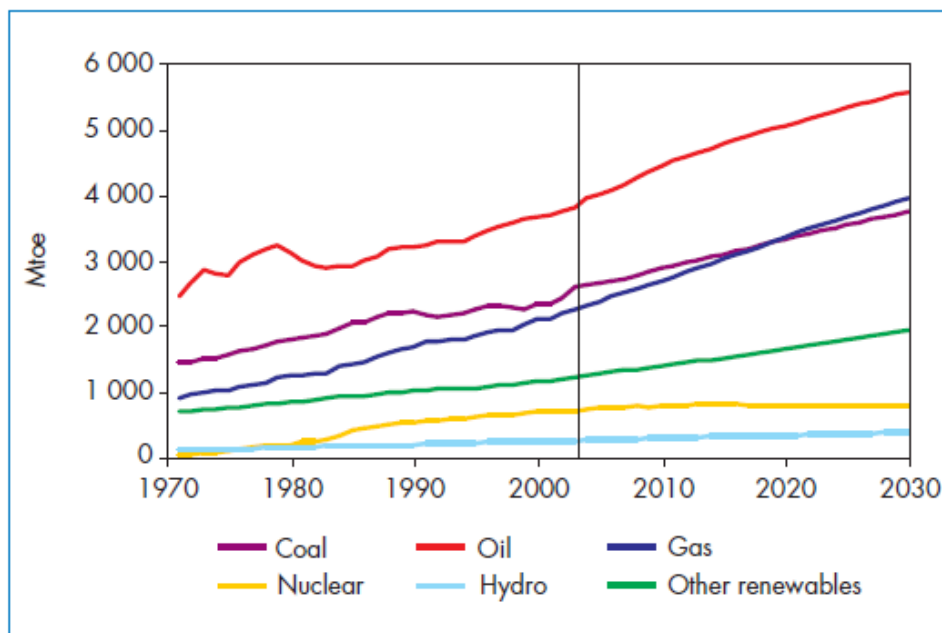


Figure 1 World primary energy demand by fuel [2].

Oil will remain the most used source of primary energy, due to its clear advantages and qualities regarding, extractability, transportability, versatility, and cost. (Table 1)

Table 1 World primary energy demand (Mtoe) [2].

	1971	2003	2010	2020	2030
Coal	1 439	2 582	2 860	3 301	3 724
Oil	2 446	3 785	4 431	5 036	5 546
Gas	895	2 244	2 660	3 338	3 942
Nuclear	29	687	779	778	767
Hydro	104	227	278	323	368
Biomass and waste	683	1 143	1 273	1 454	1 653
Other renewables	4	54	107	172	272
Total	5 600	10 723	12 389	14 402	16 271

1. Biofuels

With the increase of the oil price and its excessive consumption, the depletion of oil resources and the evident climate change derived from the excessive use of fossil fuels, the development of alternative fuels based on renewable energy sources became necessary [4, 5].

In the short term, biofuels produced from renewable raw materials, are the only alternative energy source that can effectively replace the oil-based fuels in many applications.

Biofuels are renewable fuels, biodegradable, nontoxic and essentially free of sulphur and aromatics, and are produced from organic matter such as biomass. They can be solid, liquid or gaseous [6, 7].

There are a variety of biofuels potentially available, such as bioethanol, biomethanol, biogas, bio-syngas, biodiesel, biohydrogen, but the main biofuels being considered globally are biodiesel and bioethanol [8].

Bioethanol and biodiesel are two biofuels that might replace gasoline and diesel fuel, respectively, since, they have similar physical and chemical properties, and so, can be used without major changes in classical combustion engines. These may also reduce considerably our dependence on oil, as transportation is one of the main energy consuming

sectors. As blends or by themselves, biofuels can help to reduce substantially both oil imports and carbon emissions to the atmosphere.

The production of these biofuels has increased in recent years, and projections indicate that growth is expected to continue over time, as is shown on figure 2.

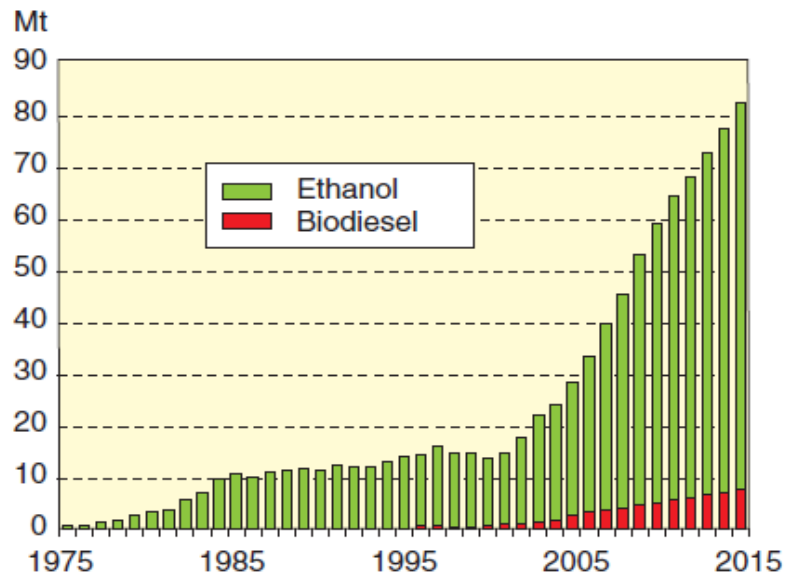


Figure 2 Trend in world biofuel production [9].

Biodiesel is produced mainly in the Europe Union, principally Germany, while bioethanol is produced and consumed mainly in Brazil and North America. However, other countries, also started to increase their production of biofuels [10].

Biodiesel and bioethanol can be produced from many raw materials (Figure 3). Bioethanol can be produced from a number of crops, including sugar beet, maize, wheat, potatoes, etc. Biodiesel can be produced from vegetable oils, animal fats, recycled waste vegetable oils, among others [8, 11].

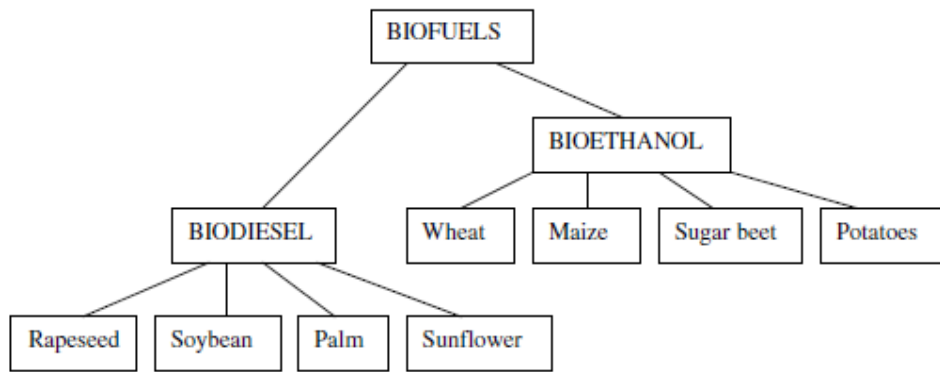


Figure 3 Some raw materials for bioethanol and biodiesel [11].

1.1 Bioethanol

1.1.1 Bioethanol production

Bioethanol is a fuel produced from many renewable feedstock sources, usually plants, such as sugar cane, sugar beet, maize (corn), wheat, and wood. These feedstock sources can be divided into sugary, starchy and lignocellulosic [6, 8, 12].

- Sugary feedstock [6, 8, 12]

Sugar beet, sugarcane and sweet sorghum are the main sugar feedstocks to produce ethanol, since these sources contain high percents of sugars.

Raw materials containing sugars can be transformed into glucose. Glucose can then be converted to ethanol and carbon dioxide, under anaerobic conditions, with the chemical reaction of this conversion is being described below:



Fungi, bacteria, and yeast can be used for the fermentation process, however, *Saccharomyces cerevisiae* is the most used yeast.

Sugarcane is the most significant crop for production of bioethanol.

- Starchy feedstock [6, 8, 12]

Corn, wheat, potatoes, barley, rice and sorghum grains are the main feedstocks containing starch.

To convert starch in to ethanol, the polymer of α -glucose is converted into glucose, through an enzymatic hydrolysis reaction. This reaction is followed by a fermentation to yield ethanol.

Corn is the dominant feedstock in industry that converts starch to ethanol, since it is composed of about 60-70% of starch.

- Lignocellulosic feedstock [6, 8, 12]

Lignocellulosic materials are the most abundant sources of carbohydrates in the Earth, and are mainly composed of cellulose, hemicelluloses and lignin. Agricultural wastes, forest residues, municipal solid wastes and wastes from pulp/paper production are the most important lignocellulosic feedstocks that can be used to produce ethanol.

Several studies have been developed for processing lignocellulosics to obtain ethanol. Although, these are not yet applicable in large scale, since the processing of these feedstocks is highly complex.

In 2017, it is estimated that the production of ethanol will increase more than twice when compared to 2007, where 127 billion litres will be produced compared with 62 billion litres in 2007 [13].

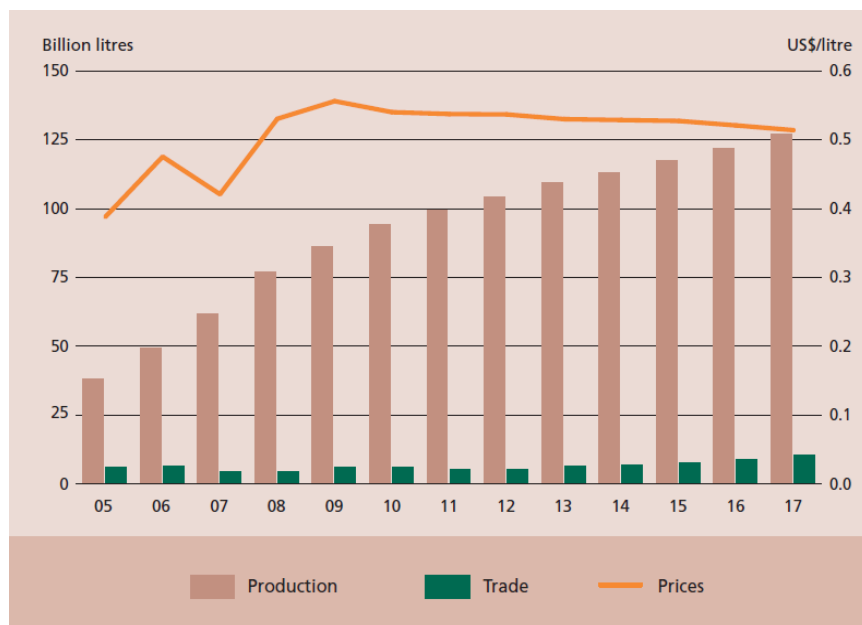


Figure 4 World bioethanol production, trade and prices, with projections to 2017.[13]

The selection of the most appropriate feedstock for ethanol production depends on the local conditions. The major problems in bioethanol production are the availability of feedstocks and their prices. In Brazil and in most tropical countries, sugar cane is the most common feedstock for ethanol production while in Europe, sugar beet and starchy materials are the most used feedstocks [14].

1.1.2 Ethanol recovery

Ethanol produced by fermentation results in a solution of ethanol in water. For ethanol to be used as a fuel, it must first be separated from water [15, 16].

Distillation is the method most used for this separation, although requiring considerable energy. This method in spite of having many advantages, has the disadvantage that ethanol purity is limited to 95-96 % due to the formation of a water-ethanol azeotrope [17].

In order to reduce the energy intensity, the chemical industry has been developing other processes for this separation, such as, adsorption, liquid-liquid extraction, pervaporation, gas stripping and steam stripping [17]. In this work, liquid-liquid extraction will be studied with more emphasis.

Liquid-liquid extraction (LLE) is a separation process that is used to separate liquid mixtures into their components, with low energy requirement. This process can be used to separate ethanol and water mixtures with a solvent, for example, purifying the products of a fermentation process [17].

There are some requisites to ensure that the extraction of ethanol-water with a solvent is a viable process, such as, high separation factor for ethanol (solvent extract preferentially ethanol than water), high selectivity for ethanol over water, low solvent solubility in the water-rich phase in to reduce the solvent losses, high capacity for ethanol to minimize the use of solvent, difference in densities between the two phases (organic and aqueous) to allow the rapid phase separation, chemical stability and effective means to recover ethanol from the solvent and recycle the solvent[18-20].

The equilibrium distribution coefficient, K_D , is the ratio of the weight fraction of ethanol or water in the organic phase to that in the aqueous phase (at equilibrium) and describes the high separation factor for ethanol [19].

$$K_{DE} = \frac{w_{E(op)}}{w_{E(ap)}} \quad (2)$$

The separation factor, α , is the ratio of the distribution coefficient of ethanol to that of water and describes the high selectivity for ethanol over water [19].

$$\alpha = \frac{K_{DE}}{K_{DW}} \quad (3)$$

Several solvents have been used to separate ethanol from water, and in previous works [21], it was found that ketones, alcohols and esters are the more suitable solvents to perform this extraction.

Castor oil and methyl laurate are possible solvents which will be studied further in this thesis.

The liquid-liquid equilibrium data are usually represented in a graph called ternary diagram. These graphs represent isotherms at a sufficient pressure to maintain the system entirely liquid. The use of these diagrams shows the phase relations in ternary liquid systems.

The compositions of these systems may be expressed in weight fraction or molar fraction. Figure 5 represents a ternary diagram of components A, B and C, at a given temperature T and pressure P.

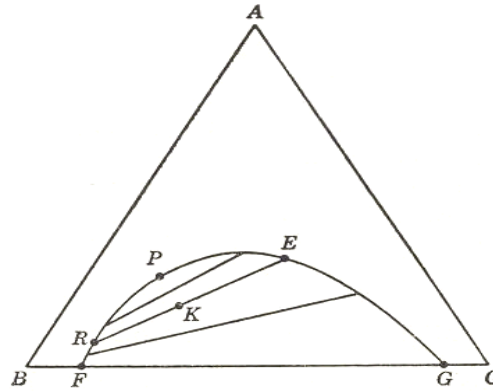


Figure 5 Ternary diagram [22].

The components (B) and (A) and (A) and (C) are completely miscible with each other, but the components (B) and (C) are only partially miscible. The saturation curve (FRPEG) separates the biphasic region from the monophasic region. The line RE is called tie-line, and represents two phases in equilibrium, resulting from an overall composition K.

1.2 Biodiesel

Conversion of the vegetable oils into biodiesel has many advantages, such as, the reduction in viscosity over vegetable oils, direct used in modern diesel engines with little or no modification and possibility of mixing with petroleum diesel fuel in any ratio. Other advantages of biodiesel are the reduction in the emissions of sulphur dioxide, carbon monoxide and hydrocarbons [23]

1.2.1 Biodiesel production

Biodiesel is produced from natural and renewable materials, such as vegetable oils and animals fats. There are four main methods to produce biodiesel: direct use and

blending, microemulsification, pyrolysis and transesterification. The most used method is the transesterification reaction [24, 25].

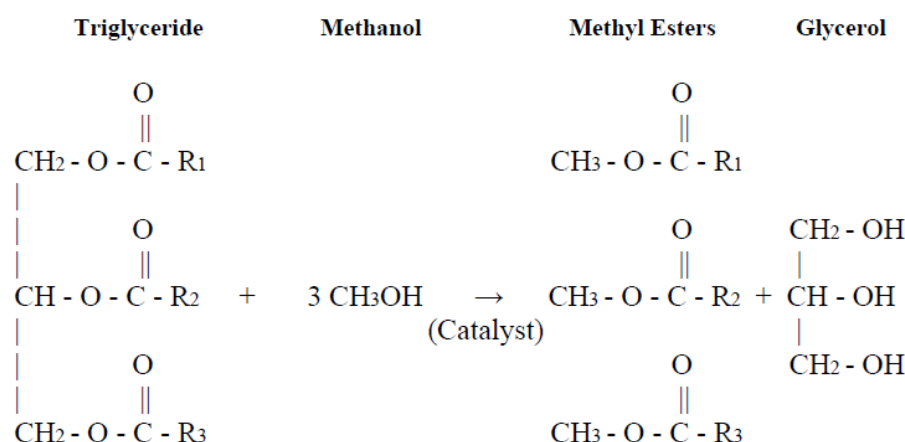


Figure 6 Transesterification reaction [26].

R1, R2, and R3 are long alkyl chains, also called fatty acid chains.

Through the transesterification reaction, vegetable oils and animal fats react with an alcohol, in the presence of a catalyst, to give the corresponding alkyl esters and glycerol. Methanol and ethanol are the most commonly used alcohols, however, methanol is preferred choice due its low cost and its physical and chemical advantages. In this reaction some types of catalysts can be employed, such as, acid, base or enzyme materials. Usually, an alkaline catalyst (sodium or potassium hydroxide) is used because the reaction is much faster than using an acid catalyst [25].

Given the reversible nature of the reaction, it is necessary to use one of the reagents in excess (alcohol) to encourage the displacement of equilibrium towards the products.

At the end of the transesterification reaction, a mixture of FAME and glycerol is obtained, however, these products have a considerable amount of excess methanol. The excess alcohol is frequently removed with a flash evaporation process or by distillation [6].

There are several variables affecting the transesterification reaction, such as catalyst, molar ratio of alcohol to oil, water content and reaction temperature, among others minor variables. If those variables are not optimized, the reaction may be incomplete and/or the yield may be significantly reduced [27].

The approximate percentage proportions of this reaction are presented in the table below:

Table 2 Biodiesel production input and output levels [28].

Process Input Levels		Process Output Levels	
Input	Volume Percentage (%)	Output	Volume Percentage (%)
Oil or Fat	87	Esther	86
Alcohol	12	Alcohol	4
Catalyst	1	Fertilizer	1
		Glycerol	9

Figure 7 shows the world biodiesel production and the projections for 2017. The production of biodiesel will grow faster than that of bioethanol, although at considerably lower level [13].

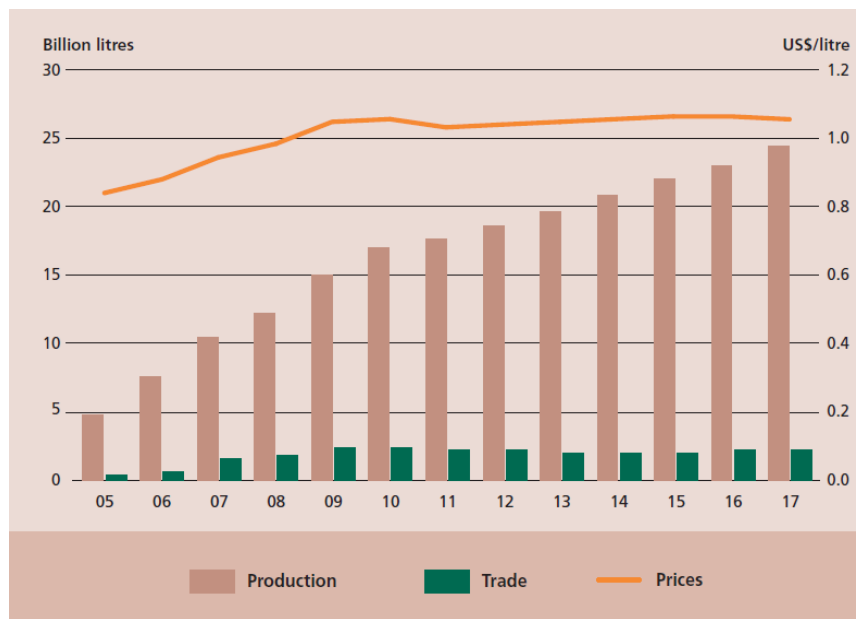


Figure 7 World biodiesel production, trade and prices, with projections to 2017 [13].

1.2.2 Biodiesel production and purification process

A simplified diagram for biodiesel production is shown in figure 8 and can be divided into various steps [29, 30]:

- *Mixing of alcohol and catalyst*: in this step the alcohol and the catalyst will be mixed, to dissolve this in the alcohol phase.

- *Transesterification reaction:* vegetable oils or animal fats are added to the previous mixture and the reaction takes place in the reactor. In Smaller plants, usually use batch reactors, but bigger plants (more than 4 million liters/year) use continuous flow processes.

- *Separation of products:* after the reaction, methyl esters and glycerol must be separated. Since glycerol is only slightly soluble in esters, this is a rapid process and can be perform in a centrifuge. Sometimes the products of the reaction need to be neutralized, which also occurs in this step.

- *Alcohol Recovery:* since each of the phases previously separated contains a large excess of alcohol used in the reaction, it is necessary to recover this alcohol. Two processes can be used to accomplish this separation, flash evaporation or distillation. However, distillation is the most used. The alcohol recovered is re-used in the process.

- *Methyl Ester wash:* following the alcohol has recovery, esters, they may suffer a process of water washing if necessary, to remove any residual catalyst, soaps, salts, methanol, or free glycerol. After this step, any remaining water is removed from the methyl esters by a vacuum flash process.

- *Glycerol neutralization:* the residual catalyst and the soaps presents in the glycerol-rich phase are neutralized with an acid. Sometimes the salts formed in this step are recovered for use as fertilizer, but in most of the cases the salts are left in the glycerol phase.

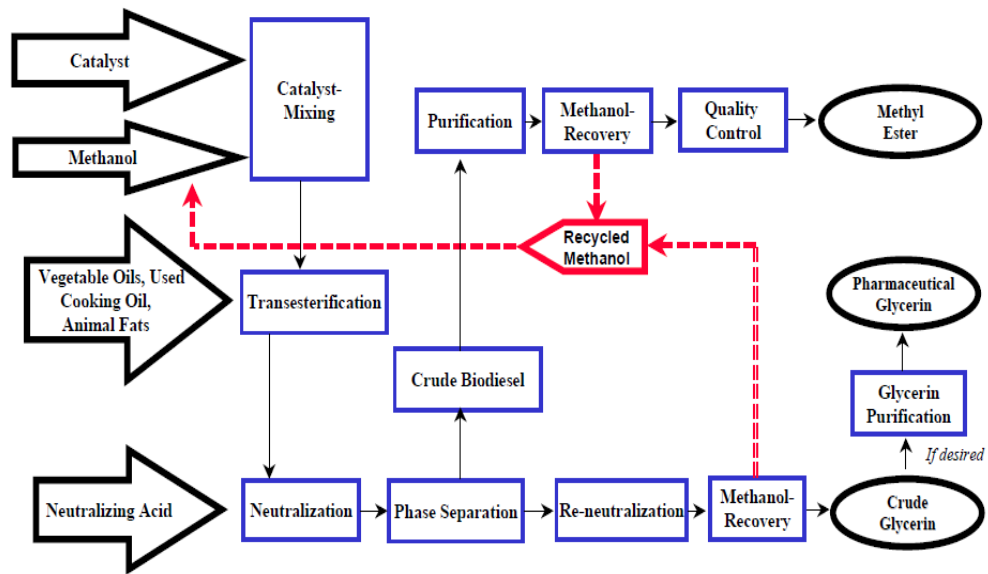


Figure 8 Diagram of biodiesel production process [29].

The knowledge of the phase equilibria of alcohol + FAME systems is thus required to design and develop the step where this separation occurs in the biodiesel production process [31, 32], and this subject will be studied on this work.

2. Model

Multi-component phase equilibria can be described using the excess Gibbs energy models (G^E), generally for low-pressure applications, and equations of state (EoS), usually for high-pressure applications.

The CPA (Cubic Plus Association) is an equation of state, that combines the Soave-Redlich-Kwong (SRK) equation of state with the association term of the Wertheim theory [33, 34]. In this equation of state the physical interactions between the molecules are described by the SRK equation, and the association term accounts for the specific site-site interactions due to hydrogen bonding and solvation effects.

Since the CPA model takes into account the interactions that can be found in mixtures of associating compounds, that makes it applicable to describe multiphase equilibria for systems containing associating components.[35]

The mixtures of water or ester and alcohols or glycerol are mixtures composed by associating components, and knowledge about the phase equilibria of these mixtures is important for the processes of production and purification of biofuels.

CPA has already been applied successfully to the modeling of the vapor–liquid equilibria (VLE) of alcohol–hydrocarbon [36] and glycol–water systems [37], the liquid–liquid equilibria (LLE) of alcohol–hydrocarbon [38], glycol–hydrocarbon [39], water–fluorocarbons [40] and water–hydrocarbon mixtures [41], VLE and LLE for ternary mixtures containing water, alcohols and alkanes [42], VLE for glycerol systems [43] and recently was also applied to describe the solid–liquid equilibria (SLE) of glycol/methanol–water systems [35].

The CPA EoS can be expressed in terms of compressibility factor as:

$$Z = Z^{phys.} + Z^{assoc.}$$

$$Z = \frac{1}{1 - b\rho} - \frac{a\rho}{RT(1 + b\rho)} - \frac{1}{2} \left(1 + \rho \frac{\partial \ln g}{\partial \rho} \right) \sum_i x_i \sum_{A_i} (1 - X_{Ai}) \quad (4)$$

where a is the energy parameter, b the co-volume, ρ is the molar density, g a simplified radial distribution function, x_i the mole fraction of the component i and X_{Ai} the mole fraction of pure i not bonded at site A [41].

X_{Ai} is related to the association strength, Δ^{AiBj} , between two sites on different molecules, site A on molecule i and site B on molecule j and is calculated by solving the following set of equations:

$$X_{Ai} = \frac{1}{1 + \rho \sum_j x_j \sum_{B_j} X_{B_j} \Delta^{AiB_j}} \quad (5)$$

The association strength Δ^{AiBj} is given by:

$$\Delta^{AiB_j} = g(\rho) \left[\exp\left(\frac{\varepsilon^{AiB_j}}{RT}\right) - 1 \right] b_{ij} \beta^{AiB_j} \quad (6)$$

Where ε^{AiB_j} is the pure component association energy, and β^{AiB_j} the pure component association volume.

The simplified radial distribution function, $g(\rho)$, is given by:

$$g(\rho) = \frac{1}{1 - 1.9\eta} \quad \text{where } \eta = \frac{1}{4} b \rho. \quad (7)$$

The energy parameter, a , for pure parameters is given by a Soave-type temperature dependency:

$$a = a_0 \left[1 + c_1 (1 - \sqrt{T_r}) \right]^2 \quad (8)$$

where T_r is the reduced temperature (T/T_c).

For non-associating components CPA has three pure component parameters (a_0 , c_1 and b) while for associating components it has five (a_0 , c_1 , b , β , ε). In both cases, these parameters are regressed simultaneously from pure component experimental data

The regression of the pure-compounds parameters is done using selected vapor pressure and liquid density data with the following objective function:

$$OF = \sum_i^{NP} \left(\frac{P_i^{\text{exp.}} - P_i^{\text{calc.}}}{P_i^{\text{exp.}}} \right)^2 + \sum_i^{NP} \left(\frac{\rho_i^{\text{exp.}} - \rho_i^{\text{calc.}}}{\rho_i^{\text{exp.}}} \right)^2 \quad (9)$$

When CPA EoS is applied to mixtures, the energy and the co-volume parameters of the physical term are calculated using the conventional van der Waals one-fluid rules:

$$a = \sum_i \sum_j x_i x_j a_{ij}, \quad \text{where } a_{ij} = \sqrt{a_i a_j} (1 - k_{ij}) \quad (10)$$

$$b = \sum_i x_i b_i. \quad (11)$$

k_{ij} a binary interaction parameter, and is estimated from equilibrium data by the objective function:

$$OF = \sum_i^{NP} \left(\frac{T_i^{\text{calc.}} - T_i^{\text{exp.}}}{T_i^{\text{exp.}}} \right)^2 \quad (12)$$

Combining rules for the association energy and volume parameters are required for extending the CPA equation of state to mixtures containing cross-associating molecules.

Some authors [44-46] proposed different sets of combining rules for $\varepsilon^{A_i B_j}$, $\beta^{A_i B_j}$ and $\Delta^{A_i B_j}$:

$$\varepsilon^{A_i B_j} = \frac{\varepsilon^{A_i B_i} + \varepsilon^{A_j B_j}}{2}, \quad \beta^{A_i B_j} = \frac{\beta^{A_i B_i} + \beta^{A_j B_j}}{2}, \quad (13) \text{ which are referred as CR-1 set}$$

$$\varepsilon^{A_i B_j} = \frac{\varepsilon^{A_i B_i} + \varepsilon^{A_j B_j}}{2}, \quad \beta^{A_i B_j} = \sqrt{\beta^{A_i B_i} \beta^{A_j B_j}}, \quad (14) \text{ which are referred as CR-2 set}$$

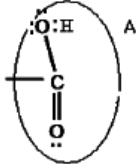
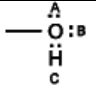
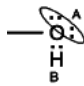
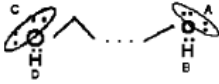
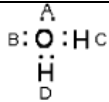
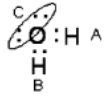
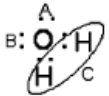
$$\varepsilon^{A_i B_j} = \sqrt{\varepsilon^{A_i B_i} \varepsilon^{A_j B_j}}, \quad \beta^{A_i B_j} = \sqrt{\beta^{A_i B_i} \beta^{A_j B_j}}, \quad (15) \text{ which are referred as CR-3 set}$$

$$\Delta^{A_i B_j} = \sqrt{\Delta^{A_i B_i} \Delta^{A_j B_j}} \quad (16) \text{ which are referred as CR-4 set (or Elliot rule)}$$

- Association scheme

The association scheme is related to the number and type of association sites for the associating compounds. There are many schemes based on the terminology of Huang and Radosz [47], which can be seen in the next table.

Table 3 Association schemes [33, 47]

Species	Formula	Type	Site fractions (X)
Acids		1A	$X_1 = X^A$
Alcohol		3B	$X^A = X^B; X^C = 2X^A - 1$ $X_1 = X^A X^B X^C$
		2B	$X^A = X^B$ $X_1 = X^A X^B$
Glycol		4C	$X^A = X^B = X^C = X^D$ $X_1 = X^A X^B X^C X^D$
Water		4C	$X^A = X^B = X^C = X^D$ $X_1 = X^A X^B X^C X^D$
		3B	$X^A = X^B; X^C = 2X^A - 1$ $X_1 = X^A X^B X^C$
		3B	$X^A = X^B; X^C = 2X^A - 1$ $X_1 = X^A X^B X^C$

Since CPA EoS is applied to mixtures containing cross-association molecules, it is necessary the use of combining rules for the association energy and volume parameters [41, 42]. In the case of ester + self associating compound systems, cross-association occurs even if the ester is not a self-associating molecule.

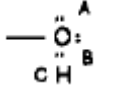
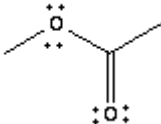
In this work, the cross-association energy parameter ($\varepsilon^{A_i B_i}$) is obtained dividing by two the energy of the associating compound (this basically means that the cross-association energy can be obtained from an arithmetic combining rule where the ε value for the ester is zero). The cross association volume is considered as an adjustable parameter, fitted to equilibrium data.

$$\varepsilon^{A_i B_i} = \frac{\varepsilon^{Associating}}{2} \quad (17) \quad \beta^{A_i B_i} \text{ (fitted)}$$

The approach followed here for the cross-association energy parameter has been successfully applied to other mixtures, such as water-aromatics or olefinics [41] and water-esters [48].

The association term depends on the number and type of association sites. For alcohols the two-site (2B) or three-site (3B) association scheme can be adopted. However, the two-site (2B) association scheme will be here used, since, both having been tested, that was the one that gave a better description of the systems [34, 47]. For the ester family a single association site is considered, cross-associating with the alcohol.

Table 4 Types of bonding in associating fluids [33, 47].

Specie	Formula	Rigorous type	Assigned type
Alcohol		3B	2B
Ester		1	1

Part II. Experimental

1. Liquid-liquid equilibria

1.1 Materials

The chemicals used to prepare the samples were castor oil, ethanol absolute and methyl laurate. Castor oil was supplied by José M. Vaz Pereira, SA, ethanol absolute was supplied by Riedel-de Haën with a purity of 99,8% and methyl laurate was supplied by Aldrich with a purity of 98%.

1.2 Experimental procedure

Ternary mixtures were prepared with compositions within the two phase region, with different amounts of water, ethanol and methyl laurate / castor oil.

Each of these samples was stirred vigorously and left to stand for 15 days in a stove at 293 K in order to achieve a good separation of phases.



Figure 9 Biphasic sample.

The method used to determine the quantity of water in each of the saturated phases was the Karl Fischer coulometry. For that purpose, a Metrohm 831 Karl Fischer Coulometer was employed.



Figure 10 Metrohm 831 Karl Fischer Coulometer.

A fixed amount of sample is added to the solution of hydranal, and it is titrated.

To determine the quantity of methyl ester / castor oil in samples a vacuum line as shown on figure 11, is used, where all the water and ethanol are removed from the sample, so that the final content of the sample is only methyl ester / castor oil.



Figure 11 Vacuum line.

The amount of ethanol is determined by the difference between the amount of water and methyl laurate / castor oil previously measured.

2. Vapor-liquid equilibria

2.1 Materials

The chemicals used in this part of work are tabulated in the next table.

Table 5 Specifications of the chemicals

Chemical	Supplier	Purity
Methanol	Lab-Scan	99,9%
Ethanol absolute	Riedel-de Haën	99,8%
Methyl laurate	Aldrich	98%
Methyl myristate	SAFC	98%
Methyl palmitate	SAFC	97%
Methyl oleate	Aldrich	70%

2.2 Experimental procedure

Isobaric VLE data (T , x) at atmospheric pressure was measured using the ebulliometer presented in figure 12. The ebulliometer is composed of a boiling still with a port for liquid sampling/injection and a condenser.

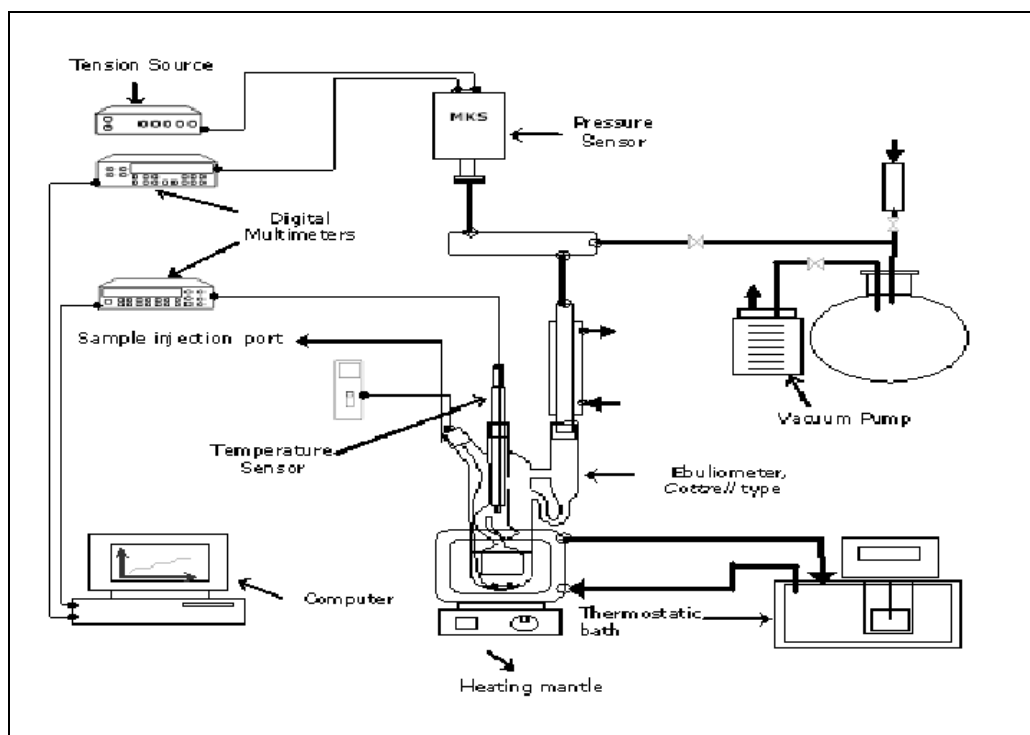


Figure 12 Ebulliometer.

The temperature control is done using a thermostatic bath. The pressure was kept constant through a vacuum line with a calibrated Baratron Heated Capacitance Manometer 728A MKS, with an accuracy of 0.50%. The total volume of the still was about 50 ml, of which about 30 ml was occupied by the liquid solution.

In the measurements a liquid solution rich in FAME was introduced into the boiling still and heated to its boiling point while mixing with a magnetic stirrer. The temperature was measured using a calibrated Pt100 temperature sensor with an uncertainty of 0.05 K, and the liquid phase sampled and its composition measured.

Subsequently fixed amounts of alcohol were introduced into the ebulliometer to change the mixture composition and the procedure repeated.

Refractive index measurements were used for analyzing the composition of the binary liquid mixtures in the boiling still, using an Abbe type refractometer, (Figure 13), with an uncertainty of 1×10^{-4} .

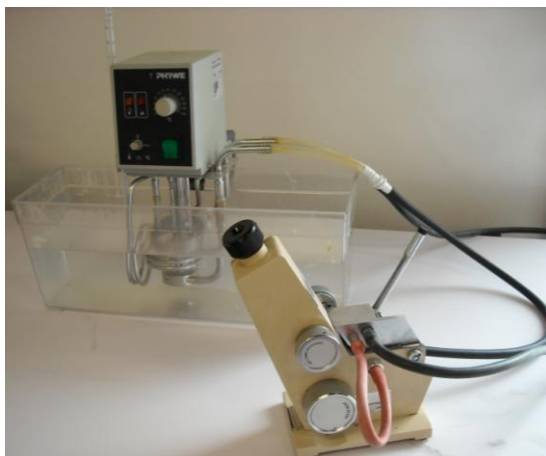


Figure 13 Abbe refractometer.

To perform the calibration curve of each system FAME + alcohol, were prepared samples with different amounts of FAME and read up the refractive indexes.

Refractive index shows a polynomial trend with the FAME weigh fraction, and using the correlation presented in figures showed at the Appendix sections A and B, it is possible to obtain the composition of the sample removed from the ebulliometer.

Part III. Results and discussion

1. Liquid-liquid equilibria

Tie lines were measured for castor oil + ethanol + water and methyl laurate + ethanol + water systems at 303K. The binodal curves (green and blue points) for these systems were already determined in another work [49]. Liquid-liquid equilibria diagrams containing binodal curves and tie lines are presented in figures below.

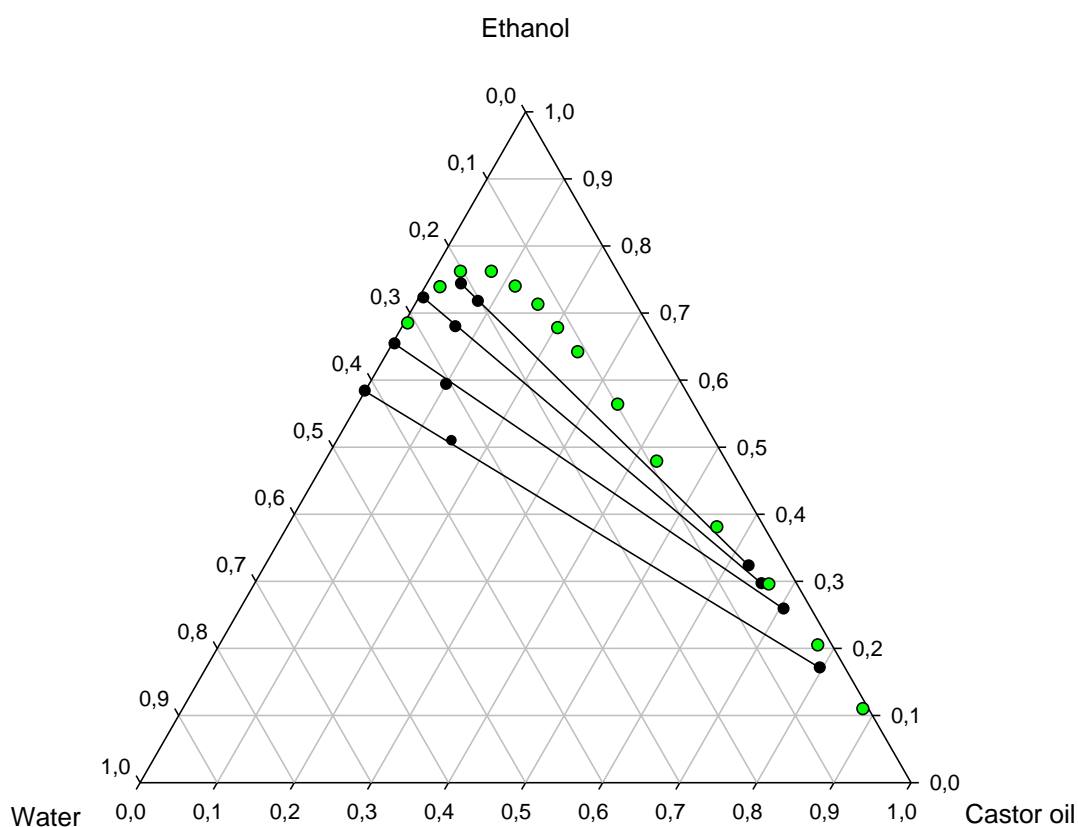


Figure 14 Ternary diagram of castor oil + ethanol + water system in weight fraction.

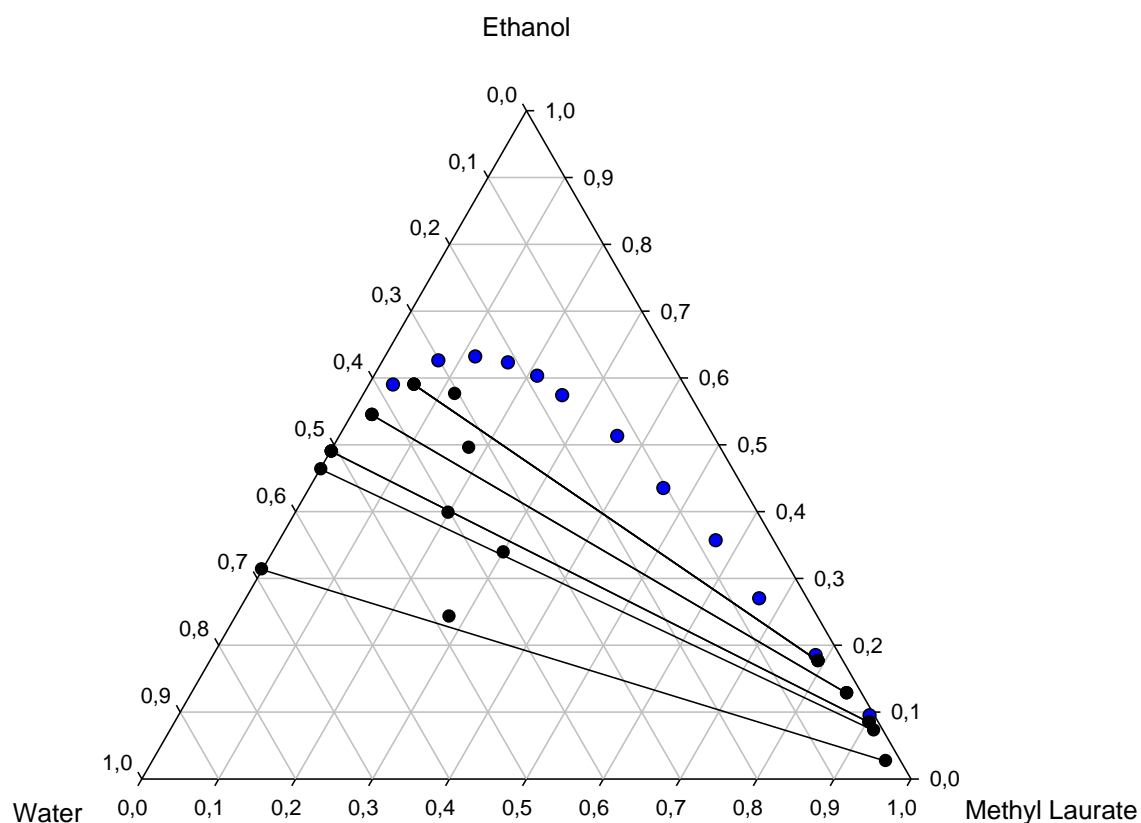


Figure 15 Ternary diagram of methyl laurate + ethanol + water system in weight fraction.

Analyzing the binodal curve of the two systems, we can see that the system water + methyl laurate + ethanol has a higher solubility because its heterogeneous region is smaller than in the ternary castor oil + ethanol + water.

The experimental tie lines data of the systems investigated are reported in the next tables.

Table 6 Tie line data for castor oil(S) + ethanol(E) + water(W) system (weight fraction).

Castor oil			Ethanol/Water Rich			Distribution		Separation
Rich Phase			Phase			coefficients		factor
w_S	w_E	w_W	w_S	w_E	w_W	K_{Dw}	K_{DE}	α
0,629	0,323	0,048	0,046	0,742	0,212	0,228	0,435	1,908
0,659	0,295	0,046	0,007	0,722	0,271	0,169	0,409	2,423
0,707	0,258	0,035	0,004	0,650	0,346	0,102	0,397	3,883
0,797	0,170	0,033	0,001	0,583	0,416	0,079	0,292	3,676

Table 7 Tie line data for methyl laurate(S) + ethanol(E) + water(W) (weight fraction).

Methyl Laurate			Ethanol/Water Rich			Distribution		Separation
Rich Phase			Phase			coefficients		factor
w_S	w_E	w_W	w_S	w_E	w_W	K_{Dw}	K_{DE}	α
0,792	0,176	0,032	0,060	0,589	0,351	0,091	0,299	3,278
0,853	0,128	0,019	0,028	0,544	0,428	0,044	0,235	5,300
0,905	0,083	0,012	0,003	0,489	0,508	0,024	0,170	7,185
0,916	0,072	0,012	0,002	0,463	0,535	0,022	0,156	6,933
0,955	0,026	0,019	0,000	0,313	0,687	0,028	0,083	3,004

Although the tie lines are not favourable, the differential miscibility of ethanol in oil and FAME and water could be exploited to separate ethanol from water.

Analyzing the experimental tie-line data, there is a low water content in the FAME/oil rich phase (organic phase) and low content of FAME/oil in the ethanol rich phase (aqueous phase). This is important in order to successfully separate ethanol from water.

As the separation factor is greater than 1, this means that the FAME and oil preferably extracts ethanol than water.

However, the low values of distribution coefficients and the separation factor, indicates that the castor oil and methyl laurate are not as good solvents for the separation as expected. Since, to be good solvents the value of α and K_{DE} should be higher.

2. Vapor-liquid equilibria

2.1 Experimental data

The measured vapor-liquid equilibria, at atmospheric pressure, for the studied systems of alcohol + methyl ester, are shown in the figures below.

- **Ethanol + methyl ester systems**

The determined boiling point temperatures for the ethanol + methyl ester systems are presented in Figures 16-19.

Analyzing the data reported in the figures, it appears that the systems studied are quite reproducible.

Any change in the composition of the mixture for fractions above 0.7 causes a sudden increase in the boiling temperature of the mixture.

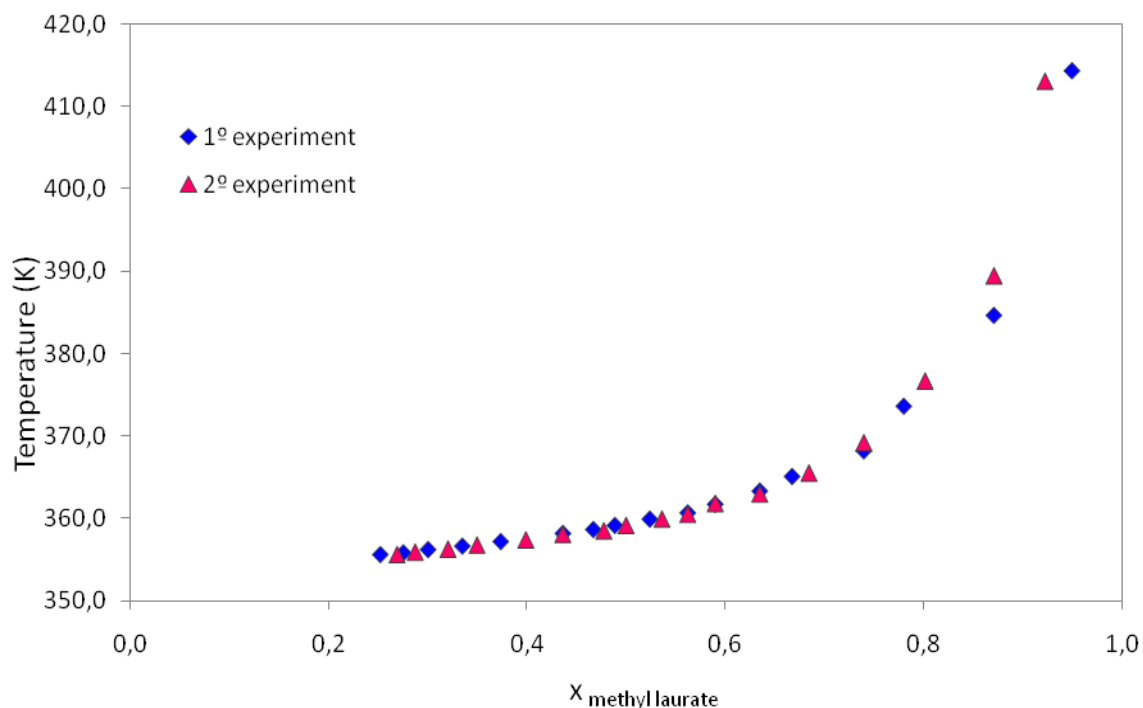


Figure 16 VLE for ethanol + methyl laurate system.

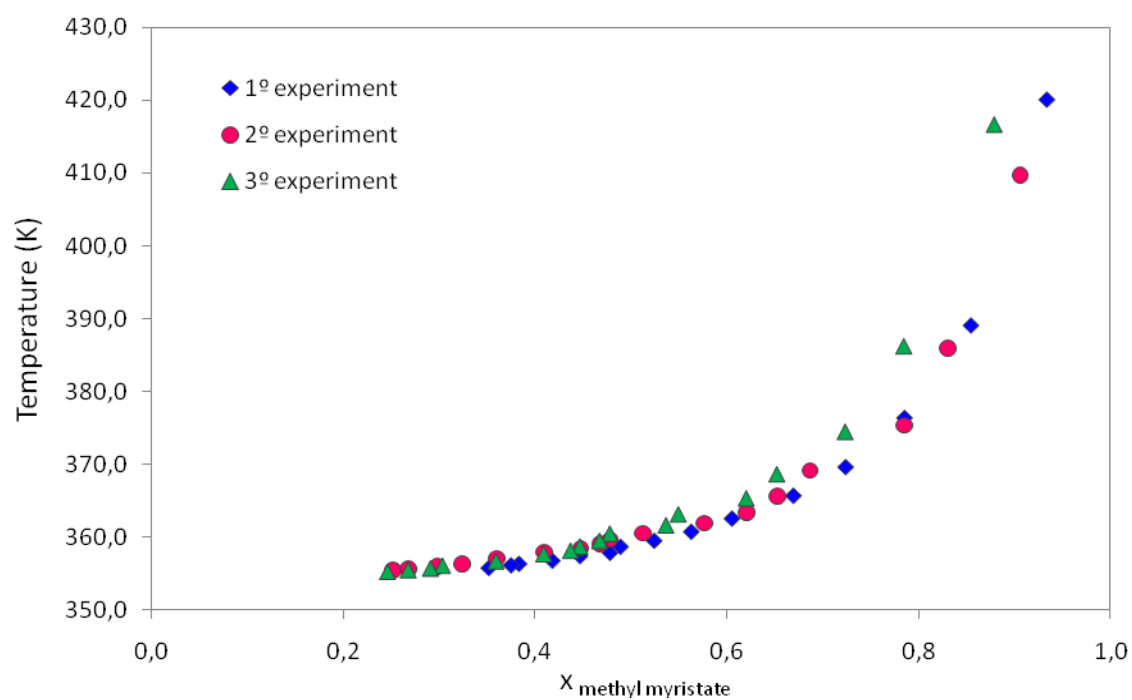


Figure 17 VLE for ethanol + methyl myristate system.

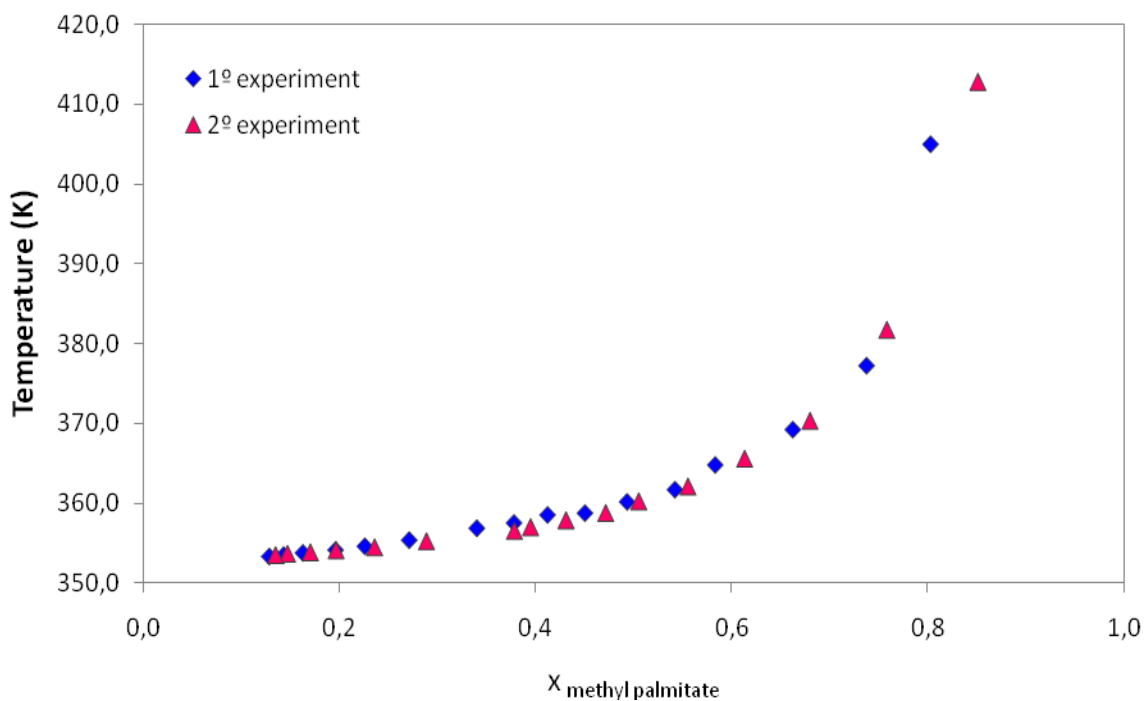


Figure 18 VLE for ethanol + methyl palmitate system.

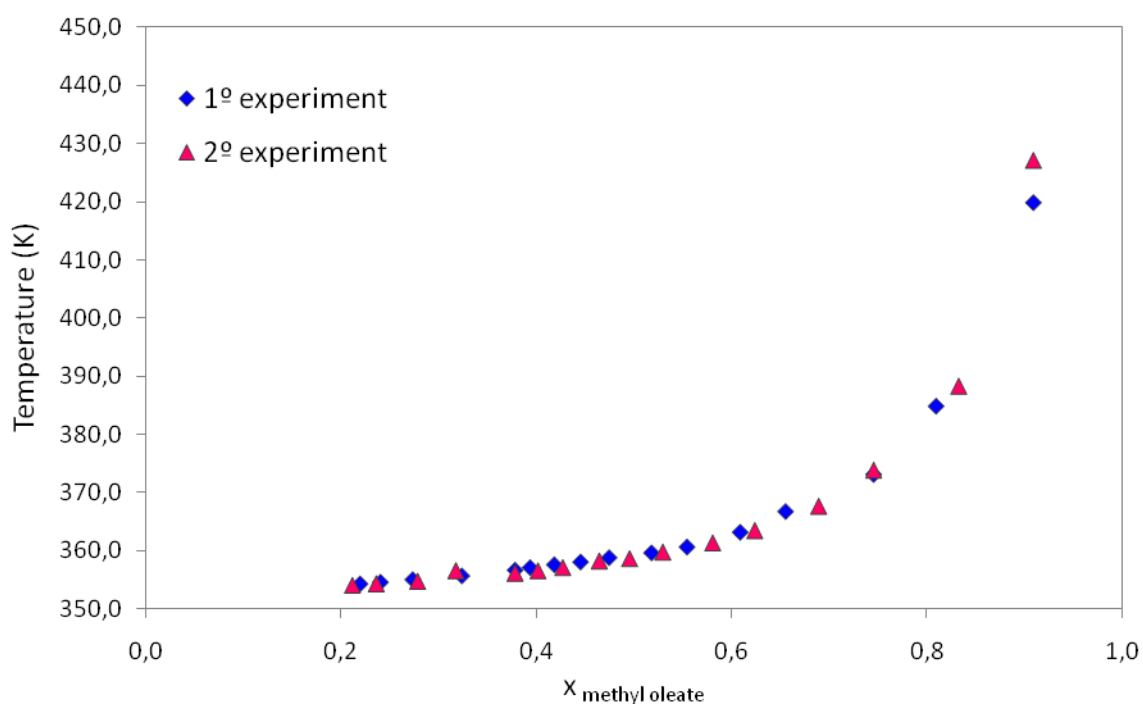


Figure 19 VLE for ethanol + methyl oleate system

- **Methanol + methyl ester systems**

Through the analysis of the boiling point plots, there is also considerable stability for these systems.

For systems methanol-methyl ester, shows that the temperature tends to stabilize quickly to molar fractions below 0.6.

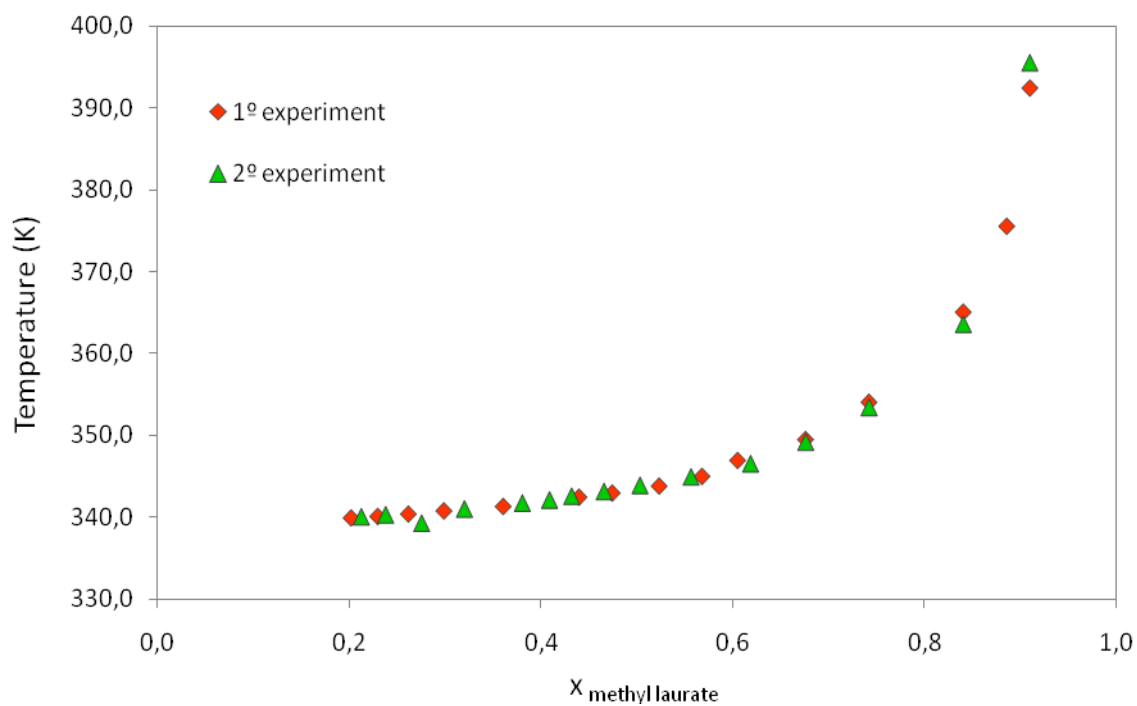


Figure 20 VLE for methanol + methyl laurate system.

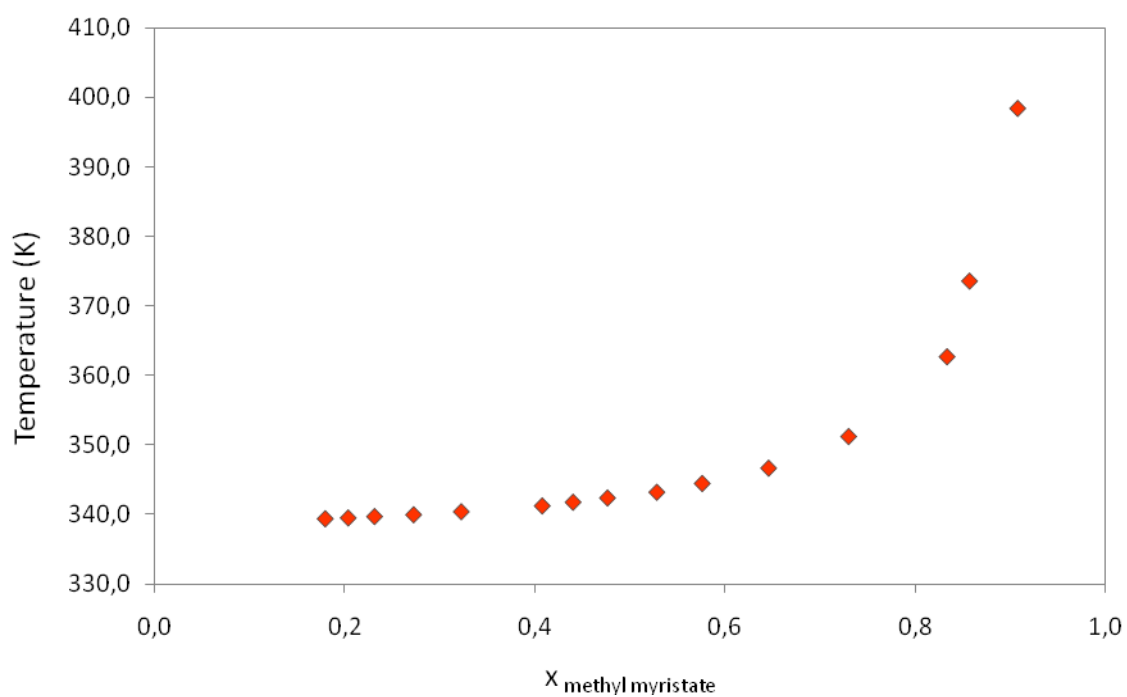


Figure 21 VLE for methanol + methyl myristate system.

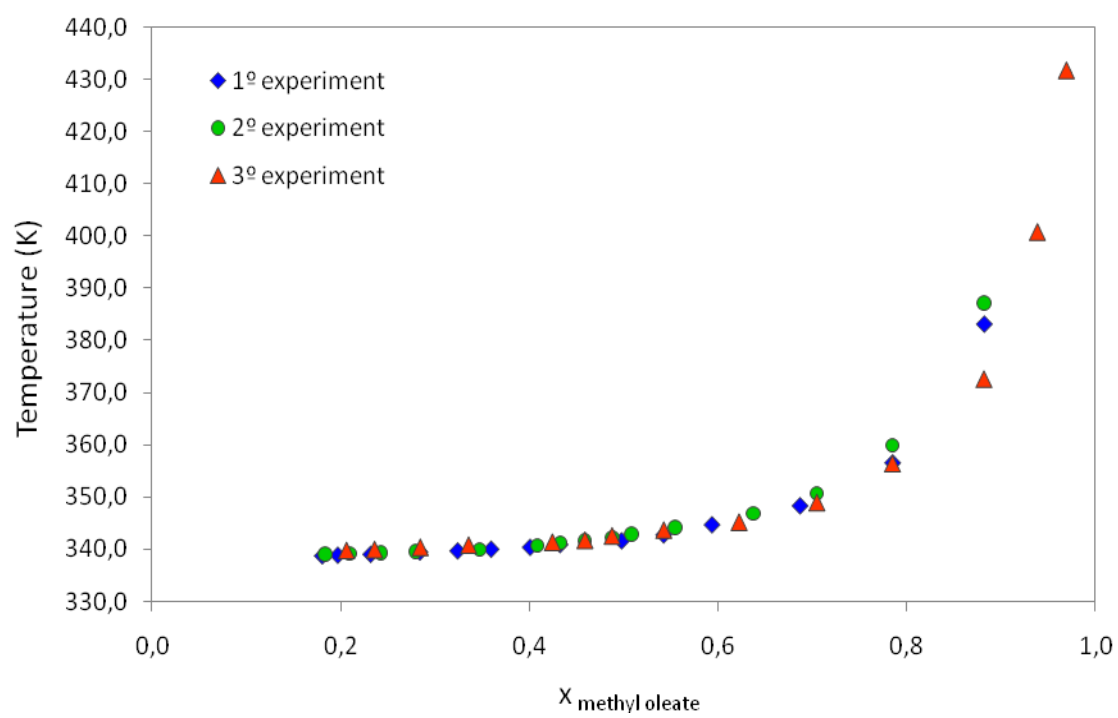


Figure 22 VLE for methanol + methyl oleate system.

2.2 Modeling

To model the new experimental data the Cubic-Plus-Association equation of state was used.

In the next table, CPA pure compounds parameters are presented. These parameters were estimated in previous works [48, 50], achieving a good description of vapor pressure and liquid densities with CPA EoS for the studied compound, with an average deviation inferior to 1% for the alcohols and 5% for the FAMES.

Table 8 CPA Pure-compound parameters and modeling results

Compound	a_0 (J.m ³ .mol ⁻²)	c_1	$b \times 10^4$ (m ³ .mol ⁻¹)	$\beta \times 10^2$	ϵ (J.mol ⁻¹)	AAD (%)	
						P^s	ρ
Methanol	0,43268	0,74696	0,32151	3,4096	20859	0,29	0,14
Ethanol	0,68415	0,93923	0,47508	1,9212	21336	0,35	0,51
Methyl laurate	7,4563	1,3712	2,4041			0,80	1,31
Methyl myristate	8,8395	1,5074	2,7951			3,66	
Methyl Oleate	10,6962	1,8649	3,3387			4,81	1,74

To calculate the average absolute deviation (AAD %) the following formula was used:

$$\left(\%AAD = \frac{1}{NP} \sum_{i=1}^{NP} ABS \left[\frac{\exp_{.i} - calc_{.i}}{\exp_{.i}} \right] \times 100 \right) \quad (17)$$

The fitting of the binary interaction parameter k_{ij} (Eq 9) is required, in order to achieve a good vapor liquid equilibria description. During the modeling of the experimental data, the β_{ij} parameter tended to a constant value: 0,10 for ethanol-FAME and 0,13 for methanol-FAME systems, with the larger value for the methanol + fame systems being explained by the stronger solvation effect of the shorter chain length alcohol. Fixing this parameter, k_{ij} will be calculated again and its value will be correlated with the ester chain length, making the model predictive for these type of systems.

Phase equilibrium data and CPA pure parameters for other ester systems, such as those with ethyl metanoate [51], methyl butanoate [52], hexyl acetate, methyl acetate [53], ethyl propionate [54] and ethyl butanoate [55] were available in the literature. They were used to estimate the parameter k_{ij} and to establish a trend for these parameters with the number of carbons of the ester compound.

The results of the regression of these binary interaction parameters are presented in the next tables and figures.

Table 9 CPA binary interaction parameters for ethanol + ester systems

$\beta_{ij} = 0,1$		
Compound	k_{ij}	AAD %
Ethyl metanoate	0,0254	0,17
Methyl butanoate	0,0190	0,15
Hexyl acetate	0,0129	0,53
Methyl laurate	-0,0002	0,33
Methyl myristate	-0,0046	0,11
Methyl oleate	-0,0197	0,34

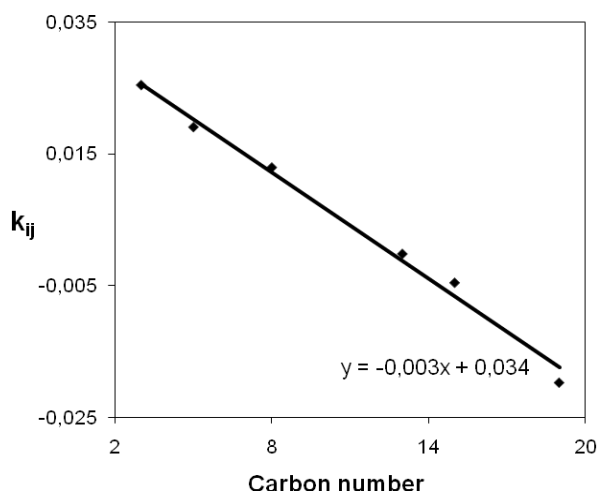
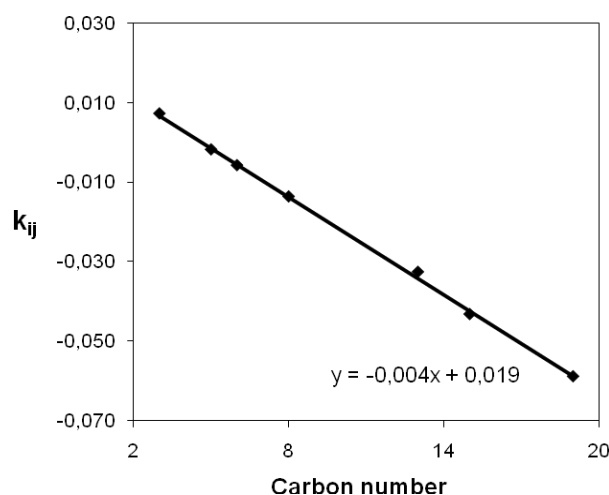


Figure 23 k_{ij} trend with the ester carbon number for ethanol + ester systems.

Table 10 CPA binary interaction parameters for methanol + ester systems

$\beta_{ij}=0,13$		
Compound	k_{ij}	AAD%
Ethyl propionate	-0,0019	0,15
Methyl acetate	0,0072	0,03
Hexyl acetate	-0,0137	0,41
Ethyl butanoate	-0,0058	0,54
Methyl laurate	-0,0326	0,27
Methyl meristate	-0,0432	0,39
Methyl oleate	-0,0589	0,41

**Figure 24** k_{ij} trend with the ester carbon number for methanol + ester systems

Comparing figures 23 and 24, it clear that the k_{ij} 's shows a linear trend with the number of carbons in the ester chain. So, using the correlations presented in the figures and the β_{ij} values presented before, the use of the CPA equation of state to describe these VLE can be performed in a totally predictive way.

In the following figures the CPA results are presented for the different studied systems.

- **Ethanol + methyl ester systems**

In the figures below, the experimental data are described by the CPA EoS.

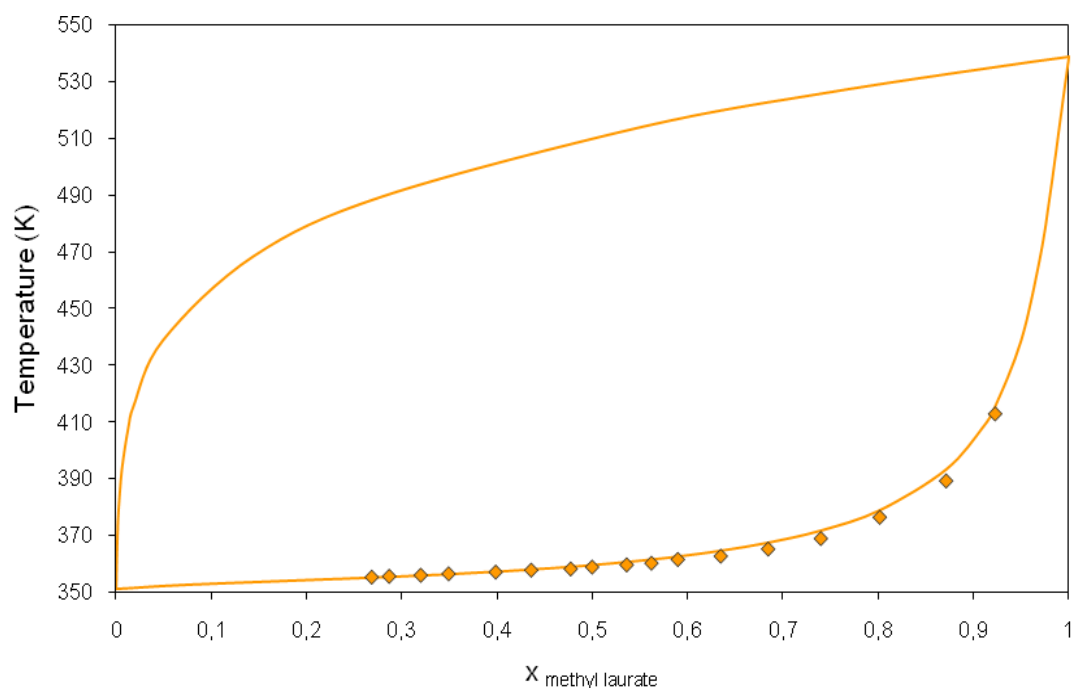


Figure 25 VLE for ethanol + methyl laurate system with $k_{ij}=-0,0002$.

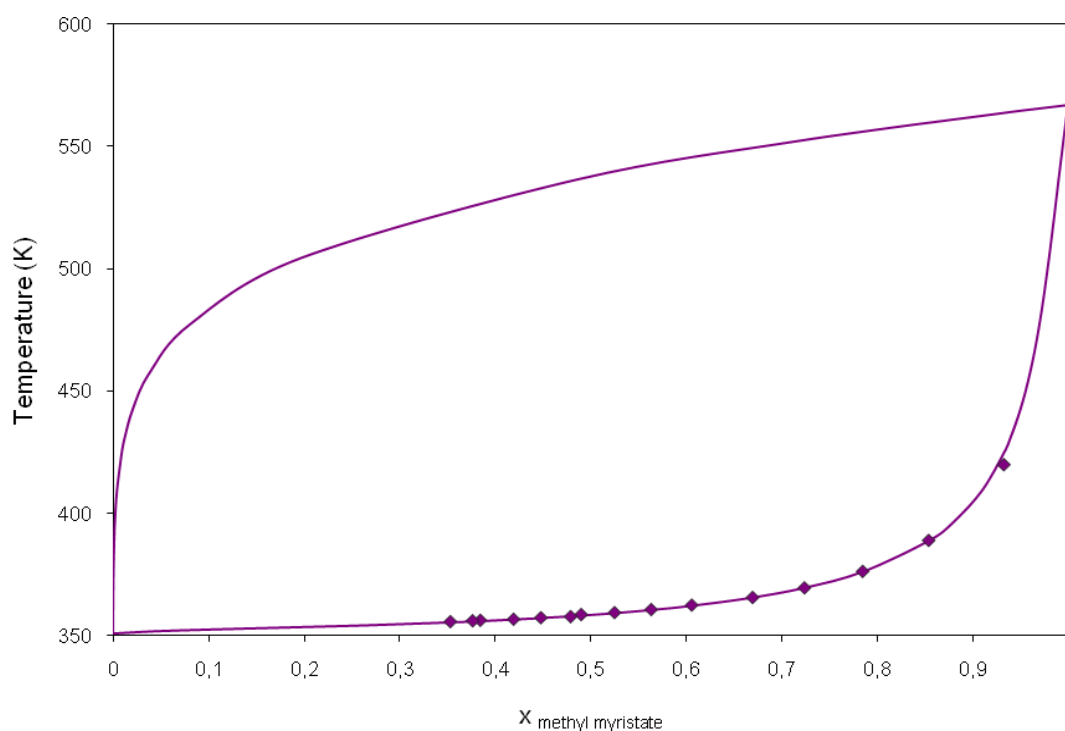


Figure 26 VLE for ethanol + methyl myristate system with $k_{ij}=-0,0046$.

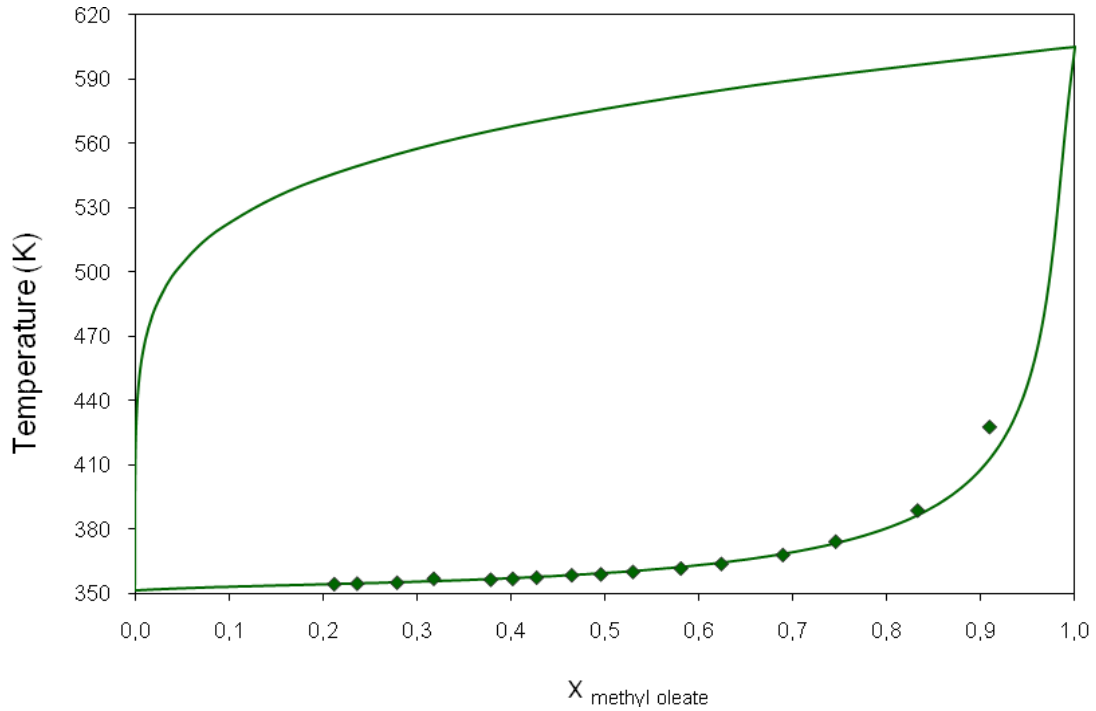


Figure 27 VLE for ethanol + methyl oleate system with $k_{ij}=-0,0197$.

In this work, a two-site (2B) association scheme was adopted for alcohols. For the ester family a single association site is considered, cross-associating with the alcohol.

With the k_{ij} and β_{ij} parameters obtained before, the vapor-liquid equilibria was correctly estimated by the CPA equation of state.

Comparing the figures, it appears that the CPA equation of state provides very good results for the three ethanol + FAME systems, especially for ester compositions smaller than 0,8.

- **Methanol + methyl ester systems**

In the next figures, the experimental data are described by the CPA EoS

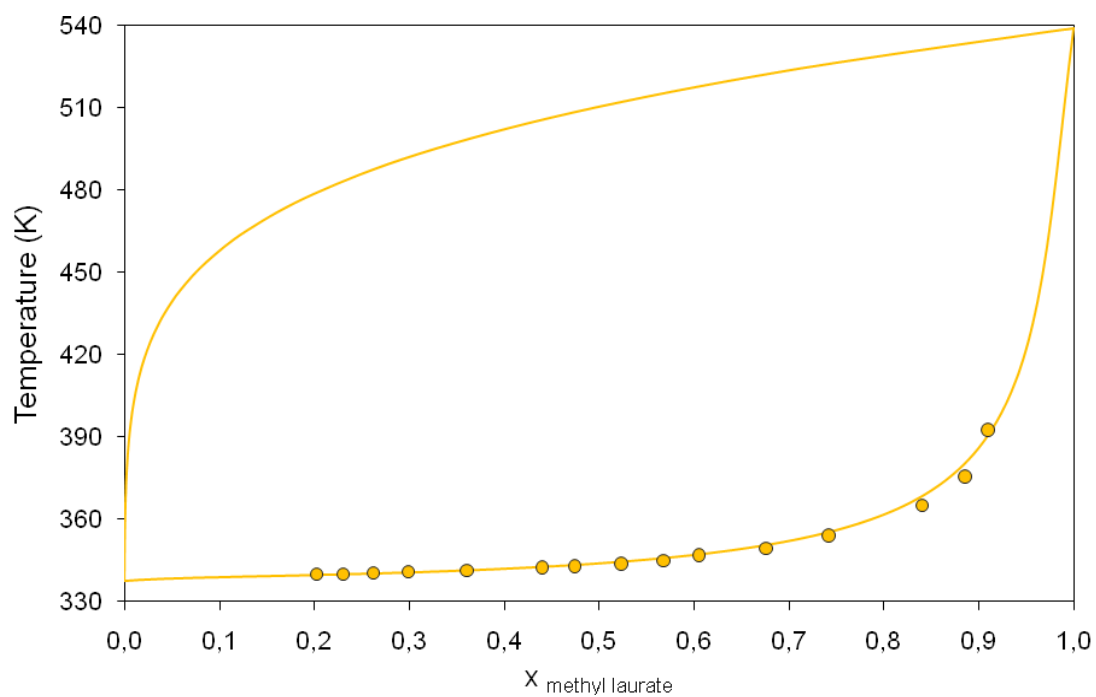


Figure 28 VLE for methanol + methyl laurate system with $k_{ij}=-0,0326$.

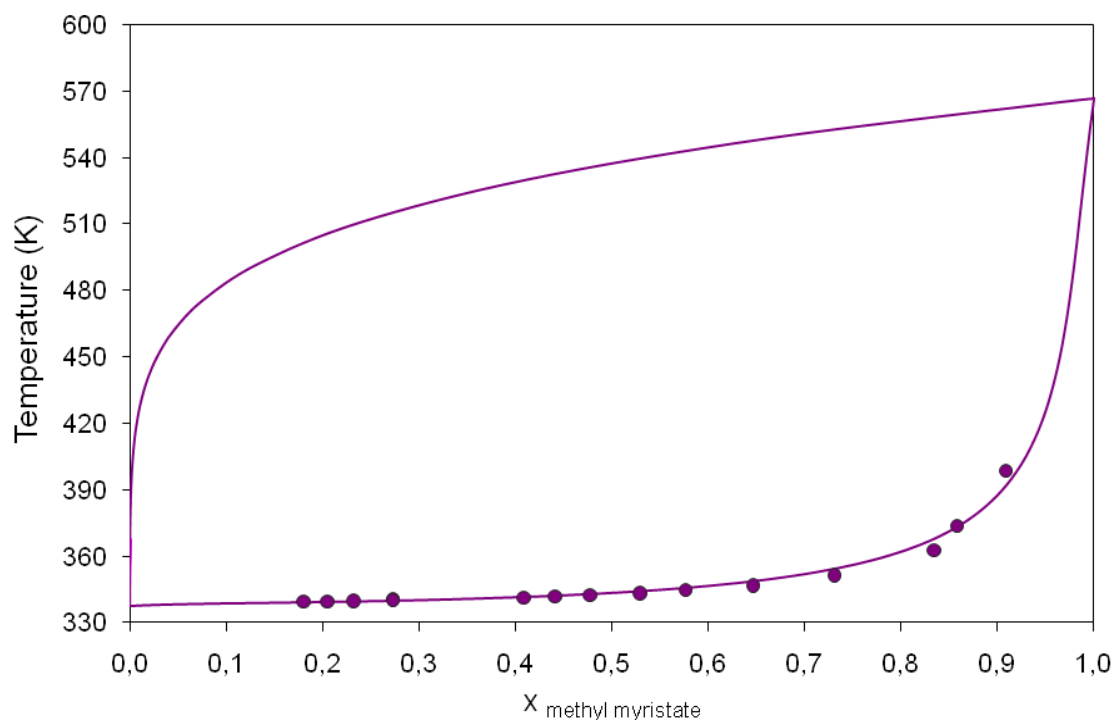


Figure 29 VLE for methanol + methyl myristate system with $k_{ij}=-0,0432$.

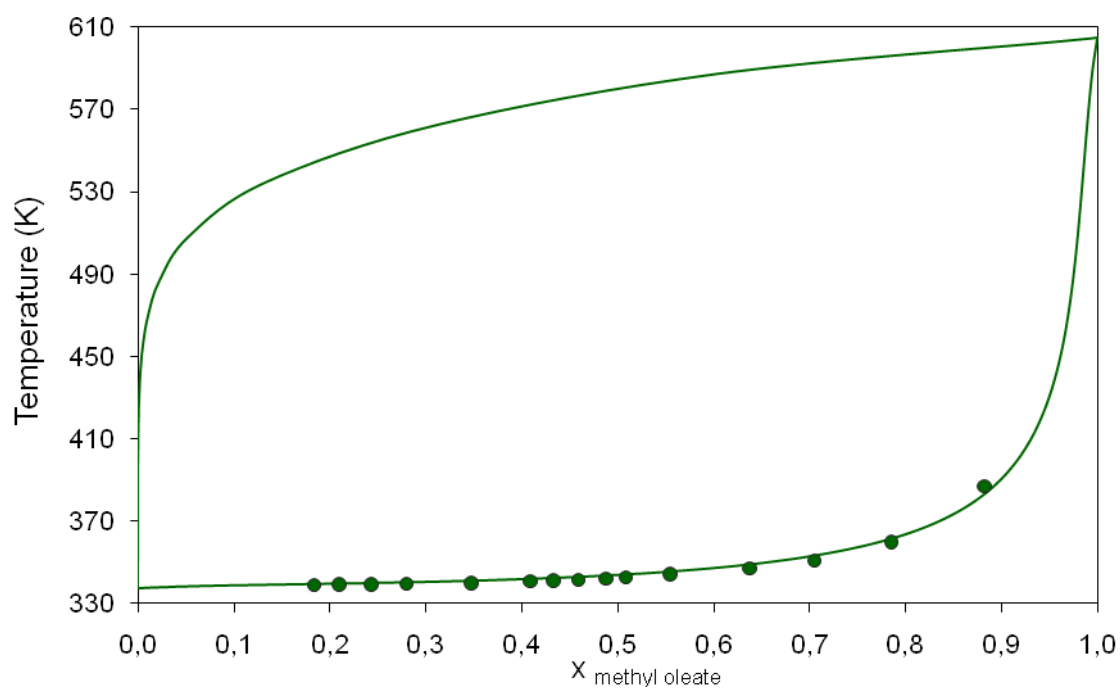


Figure 30 VLE for methanol + methyl oleate system with $k_{ij}=-0,0589$.

The results obtained from the CPA equation of state are again, as for the previous ethanol + FAME systems, in very good agreement with the experimental VLE, being only necessary a single, small and temperature independent binary interaction parameter, with these being dependent on the ester chain length.

Comparing the systems ethanol-FAME and methanol-FAME, they exhibit the same behaviour, differing only in temperature, which in the case of ethanol-FAME is higher.

It was important to measure the VLE for FAME + alcohols systems, since these kind of data was surprisingly scarce in the literature and the knowledge of these phase equilibria is an important step for designing and developing the biodiesel purification processes.

Once CPA EoS has been already applied successfully for other systems in biodiesel production and purification [43], it was a relevant fact that to confirm in this work that the application of this equation continues to be valid for describing other systems of importance for the biodiesel industry.

Part IV. Conclusions

The production of biofuels has increased substantially over the years, with particular importance to biodiesel and bioethanol.

Bioethanol produced by fermentation, results in a solution of ethanol in water. This solution can be separated using various techniques. Liquid-liquid extraction is an alternative method and requires less energy to operate than conventional methods, such as distillation.

In this work the liquid-liquid equilibria for water-ethanol-methyl ester/ oil systems was studied, in order to evaluate which was the best solvent to carry out the separation of ethanol from water. Castor oil and methyl laurate were evaluated for their ability for this separation. Although the obtained values for the separation factor are greater than 1, the distribution coefficients values are relatively low. This means that the castor oil and methyl laurate are not good solvents to perform an efficient separation.

The vapor-liquid equilibria for alcohols + FAMES were measured at atmospheric pressure, since the knowledge of the phase equilibria is an important factor and is required to design and develop the biodiesel production and purification processes.

The CPA (Cubic-Plus-Association) equation of state was successfully applied to model the new VLE experimental data.

The two-site (2B) association scheme was adopted for alcohols in this work, while a single association site that interacts solely with other sites in a different associating molecule was considered for esters. This was found to be a good option for systems alcohol + esters.

A single, small, temperature independent and ester carbon number dependent binary interaction parameter was enough to obtain a very good description of the experimental VLE data. Correlations for obtaining the k_{ij} 's as a function of the ester chain length were proposed. A constant value for β_{ij} was also used, making this model totally predictive.

Part V. Bibliographic References

1. Bhima Sastri, A.L., *World Biofuels Production Potential*. 2008, U. S. Department of Energy: Washington, DC.
2. (InternationalEnergyAgency), I., *World Energy Outlook 2005*. 2005.
3. Birol, F. and Argiri, M., *World energy prospects to 2020*. Energy, 1999. **24**(11): p. 905-918.
4. Mathews, J.A., *Biofuels, climate change and industrial development: can the tropical South build 2000 biorefineries in the next decade?* Biofuels Bioproducts & Biorefining-Biofpr, 2008. **2**(2): p. 103-125.
5. Petrou, E.C. and Pappis, C.P., *Biofuels: A Survey on Pros and Cons*. Energy & Fuels, 2009. **23**(1): p. 1055-1066.
6. Pandey, A., ed. *Handbook of Plant-Based Biofuels*. 2009, Taylor & Francis Group: New York.
7. Taylor, G., *Biofuels and the biorefinery concept*. Energy Policy, 2008. **36**(12): p. 4406-4409.
8. Rutz, D.J., R., *Biofuel Technology Handbook*. 2007, Munique: WIP Renewable Energies.
9. <http://www.dupontelastomers.com/autofocus/a4/af4.asp?article=biofuels> (March 2009).
10. Demirbas, A., *Political, economic and environmental impacts of biofuels: A review*. Applied Energy. In Press, Corrected Proof.
11. Demirbas, A., *Biofuels sources, biofuel policy, biofuel economy and global biofuel projections*. Energy Conversion and Management, 2008. **49**(8): p. 2106-2116.
12. Balat, M. and Balat, H., *Recent trends in global production and utilization of bio-ethanol fuel*. Applied Energy, 2009. **86**(11): p. 2273-2282.

13. *THE STATE OF FOOD AND AGRICULTURE*. 2008, Rome: FOOD AND AGRICULTURE ORGANIZATION OF THE UNITED NATIONS.
14. Balat, M., Balat, H., and Oz, C., *Progress in bioethanol processing*. Progress in Energy and Combustion Science, 2008. **34**(5): p. 551-573.
15. Fatih Demirbas, M., *Biorefineries for biofuel upgrading: A critical review*. Applied Energy. In Press, Corrected Proof.
16. Mehta, G.D. and Fraser, M.D., *A NOVEL EXTRACTION PROCESS FOR SEPARATING ETHANOL AND WATER*. Industrial & Engineering Chemistry Process Design and Development, 1985. **24**(3): p. 556-560.
17. Vane, L.M., *Separation technologies for the recovery and dehydration of alcohols from fermentation broths*. Biofuels Bioproducts & Biorefining-Biofpr, 2008. **2**(6): p. 553-588.
18. Koullas, D.P., Umealu, O.S., and Koukios, E.G., *Solvent selection for the extraction of ethanol from aqueous solutions*. Separation Science and Technology, 1999. **34**(11): p. 2153-2163.
19. Munson, C.L. and King, C.J., *FACTORS INFLUENCING SOLVENT SELECTION FOR EXTRACTION OF ETHANOL FROM AQUEOUS-SOLUTIONS*. Industrial & Engineering Chemistry Process Design and Development, 1984. **23**(1): p. 109-115.
20. Offeman, R.D., Stephenson, S.K., Robertson, G.H., and Orts, W.J., *Solvent extraction of ethanol from aqueous solutions. I. Screening methodology for solvents*. Industrial & Engineering Chemistry Research, 2005. **44**(17): p. 6789-6796.
21. Solimo, H.N., Martinez, H.E., and Riggio, R., *LIQUID LIQUID EXTRACTION OF ETHANOL FROM AQUEOUS-SOLUTIONS WITH AMYL ACETATE, BENZYL ALCOHOL, AND METHYL ISOBUTYL KETONE AT 298.15-K*. Journal of Chemical and Engineering Data, 1989. **34**(2): p. 176-179.

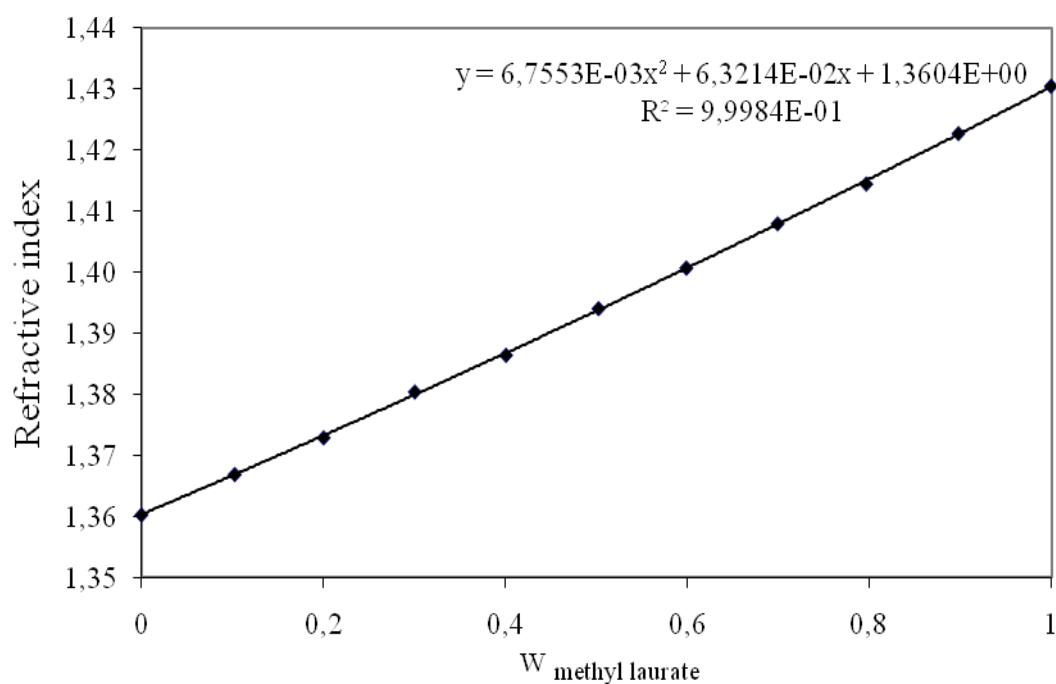
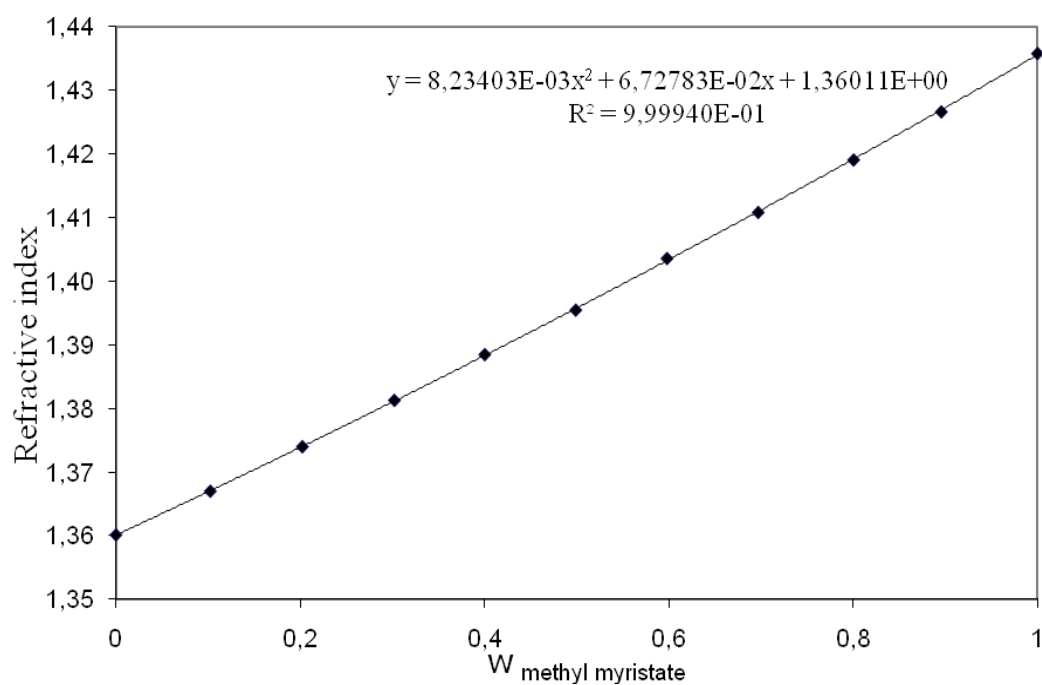
22. Gisielly Schoeffel, L.B.A., Maicon Luiz Hilgenstieler, Sharlene Schmitt, *CURVA BINODAL E LINHAS DE AMARRAÇÃO*. 2003, Universidade Regional de Blumenau: Blumenau.
23. Moser, B.R., *Biodiesel production, properties, and feedstocks*. In *Vitro Cellular & Developmental Biology-Plant*, 2009. **45**(3): p. 229-266.
24. Hegel, P., Mahe, G., Pereda, S., and Brignole, E.A., *Phase transitions in a biodiesel reactor using Supercritical methanol*. *Industrial & Engineering Chemistry Research*, 2007. **46**(19): p. 6360-6365.
25. Ma, F.R. and Hanna, M.A., *Biodiesel production: a review*. *Bioresource Technology*, 1999. **70**(1): p. 1-15.
26. Gerpen, J.V., *Biodiesel processing and production*. *Fuel Processing Technology*, 2005. **86**(10): p. 1097-1107.
27. Sharma, Y.C. and Singh, B., *Development of biodiesel: Current scenario*. *Renewable & Sustainable Energy Reviews*, 2009. **13**(6-7): p. 1646-1651.
28. http://www.biodiesel.org/pdf_files/fuelfactsheets/Production.PDF (March 2009)
29. Christian Jason M. Alfaro, H.S.d.L., Katrina P. Mendoza, Rex M. Urbiztondo, A *Comprehensive Analysis of Coco-Biodiesel Fuel*, in *School of Mechanical Engineering*. 2007, Mapúa Institute of Technology: Manila.
30. Haas, M.J., McAloon, A.J., Yee, W.C., and Foglia, T.A., *A process model to estimate biodiesel production costs*. *Bioresource Technology*, 2006. **97**(4): p. 671-678.
31. Shimoyama, Y., Iwai, Y., Abeta, T., and Arai, Y., *Measurement and correlation of vapor-liquid equilibria for ethanol + ethyl laurate and ethanol + ethyl myristate systems near critical temperature of ethanol*. *Fluid Phase Equilibria*, 2008. **264**(1-2): p. 228-234.

32. Shimoyama, Y., Iwai, Y., Jin, B.S., Hirayama, T., and Arai, Y., *Measurement and correlation of vapor-liquid equilibria for methanol + methyl laurate and methanol + methyl myristate systems near critical temperature of methanol*. Fluid Phase Equilibria, 2007. **257**(2): p. 217-222.
33. Kontogeorgis, G.M., Michelsen, M.L., Folas, G.K., Derawi, S., von Solms, N., and Stenby, E.H., *Ten years with the CPA (Cubic-Plus-Association) equation of state. Part 1. Pure compounds and self-associating systems*. Industrial & Engineering Chemistry Research, 2006. **45**(14): p. 4855-4868.
34. Kontogeorgis, G.M., Michelsen, M.L., Folas, G.K., Derawi, S., von Solms, N., and Stenby, E.H., *Ten years with the CPA (Cubic-Plus-Association) equation of state. Part 2. Cross-associating and multicomponent systems*. Industrial & Engineering Chemistry Research, 2006. **45**(14): p. 4869-4878.
35. Folas, G.K., Gabrielsen, J., Michelsen, M.L., Stenby, E.H., and Kontogeorgis, G.M., *Application of the cubic-plus-association (CPA) equation of state to cross-associating systems*. Industrial & Engineering Chemistry Research, 2005. **44**(10): p. 3823-3833.
36. Yakoumis, I.V., Kontogeorgis, G.M., Voutsas, E.C., and Tassios, D.P., *Vapor-liquid equilibria for alcohol/hydrocarbon systems using the CPA Equation of state*. Fluid Phase Equilibria, 1997. **130**(1-2): p. 31-47.
37. Derawi, S.O., Kontogeorgis, G.M., Michelsen, M.L., and Stenby, E.H., *Extension of the cubic-plus-association equation of state to glycol-water cross-associating systems*. Industrial & Engineering Chemistry Research, 2003. **42**(7): p. 1470-1477.
38. Voutsas, E.C., Kontogeorgis, G.M., Yakoumis, I.V., and Tassios, D.P., *Correlation of liquid-liquid equilibria for alcohol/hydrocarbon mixtures using the CPA equation of state*. Fluid Phase Equilibria, 1997. **132**(1-2): p. 61-75.
39. Derawi, S.O., Michelsen, M.L., Kontogeorgis, G.M., and Stenby, E.H., *Application of the CPA equation of state to glycol/hydrocarbons liquid-liquid equilibria*. Fluid Phase Equilibria, 2003. **209**(2): p. 163-184.

40. Oliveira, M.B., Freire, M.G., Marrucho, I.M., Kontogeorgis, G.M., Queimada, A.J., and Coutinho, J.A.P., *Modeling the liquid-liquid equilibria of water plus fluorocarbons with the cubic-plus-association equation of state*. Industrial & Engineering Chemistry Research, 2007. **46**(4): p. 1415-1420.
41. Folas, G.K., Kontogeorgis, G.M., Michelsen, M.L., and Stenby, E.H., *Application of the cubic-plus-association (CPA) equation of state to complex mixtures with aromatic hydrocarbons*. Industrial & Engineering Chemistry Research, 2006. **45**(4): p. 1527-1538.
42. Voutsas, E.C., Yakoumis, I.V., and Tassios, D.P., *Prediction of phase equilibria in water/alcohol/alkane systems*. Fluid Phase Equilibria, 1999. **158-160**: p. 151-163.
43. Oliveira, M.B., Teles, A.R.R., Queimada, A.J., and Coutinho, J.A.P., *Phase equilibria of glycerol containing systems and their description with the Cubic-Plus-Association (CPA) Equation of State*. Fluid Phase Equilibria, 2009. **280**(1-2): p. 22-29.
44. Fu, Y.H. and Sandler, S.I., *A SIMPLIFIED SAFT EQUATION OF STATE FOR ASSOCIATING COMPOUNDS AND MIXTURES*. Industrial & Engineering Chemistry Research, 1995. **34**(5): p. 1897-1909.
45. Suresh, J.B., E. J., *Prediction of Liquid-Liquid Equilibria in Ternary Mixtures from Binary Data*. Fluid Phase Equilibria, 1994. **99**: p. 219-240.
46. Suresh, S.J. and Elliott, J.R., *MULTIPHASE EQUILIBRIUM-ANALYSIS VIA A GENERALIZED EQUATION OF STATE FOR ASSOCIATING MIXTURES*. Industrial & Engineering Chemistry Research, 1992. **31**(12): p. 2783-2794.
47. Huang, S.H. and Radosz, M., *EQUATION OF STATE FOR SMALL, LARGE, POLYDISPERSE, AND ASSOCIATING MOLECULES*. Industrial & Engineering Chemistry Research, 1990. **29**(11): p. 2284-2294.

48. Oliveira, M.B., Varanda, F.R., Marrucho, I.M., Queimada, A.J., and Coutinho, J.A.P., *Prediction of water solubility in biodiesel with the CPA equation of state*. Industrial & Engineering Chemistry Research, 2008. **47**(12): p. 4278-4285.
49. Carvalho, S.A.d.E.S., *Equilíbrio Líquido-líquido na Produção de Biodiesel*, in *Departamento de Química*. 2007, Universidade de Aveiro: Aveiro.
50. Oliveira, M.B., Marrucho, I.M., Coutinho, J.A.P., and Queimada, A.J., *Surface tension of chain molecules through a combination of the gradient theory with the CPA EoS*. Fluid Phase Equilibria, 2008. **267**(1): p. 83-91.
51. Soto, A., Hernández, P., and Ortega, J., *Experimental VLE at 101.32 kPa in binary systems composed of ethyl methanoate and alkan-1-ols or alkan-2-ols and treatment of data using a correlation with temperature-dependent parameters*. Fluid Phase Equilibria, 1998. **146**(1-2): p. 351-370.
52. Ortega, J., Susjal, P., and Dealfonso, C., *ISOBARIC VAPOR-LIQUID-EQUILIBRIUM OF METHYL BUTANOATE WITH ETHANOL AND 1-PROPANOL BINARY-SYSTEMS*. Journal of Chemical and Engineering Data, 1990. **35**(2): p. 216-219.
53. Tu, C.H., Wu, Y.S., and Liu, T.L., *Isobaric vapor-liquid equilibria of the methanol, methyl acetate and methyl acrylate system at atmospheric pressure*. Fluid Phase Equilibria, 1997. **135**(1): p. 97-108.
54. Jos M. Resa, C.G., Salom Ortiz de Landaluce, Juan Lanz, *Density, Refractive Index, Speed of Sound, and Vapor-Liquid Equilibria for Binary Mixtures of Methanol + Ethyl Propionate and Vinyl Acetate + Ethyl Propionate*. Journal of Chemical & Engineering Data, 2002. **47**: p. 435-440.
55. Jos M. Resa, C.G., Salom Ortiz de Landaluce, Juan Lanz, *Density, Refractive Index, and Speed of Sound at 298.15 K, and Vapor-Liquid Equilibria at 101.3 kPa for Binary Mixtures of Methanol + Ethyl Butyrate and Vinyl Acetate + Ethyl Butyrate*. 2002. **47**: p. 1123-1127.

Appendix

A. Calibration curves for ethanol + FAME systems**Figure A 1** Calibration curve of ethanol + methyl laurate system.**Figure A 2** Calibration curve of ethanol + methyl myristate system.

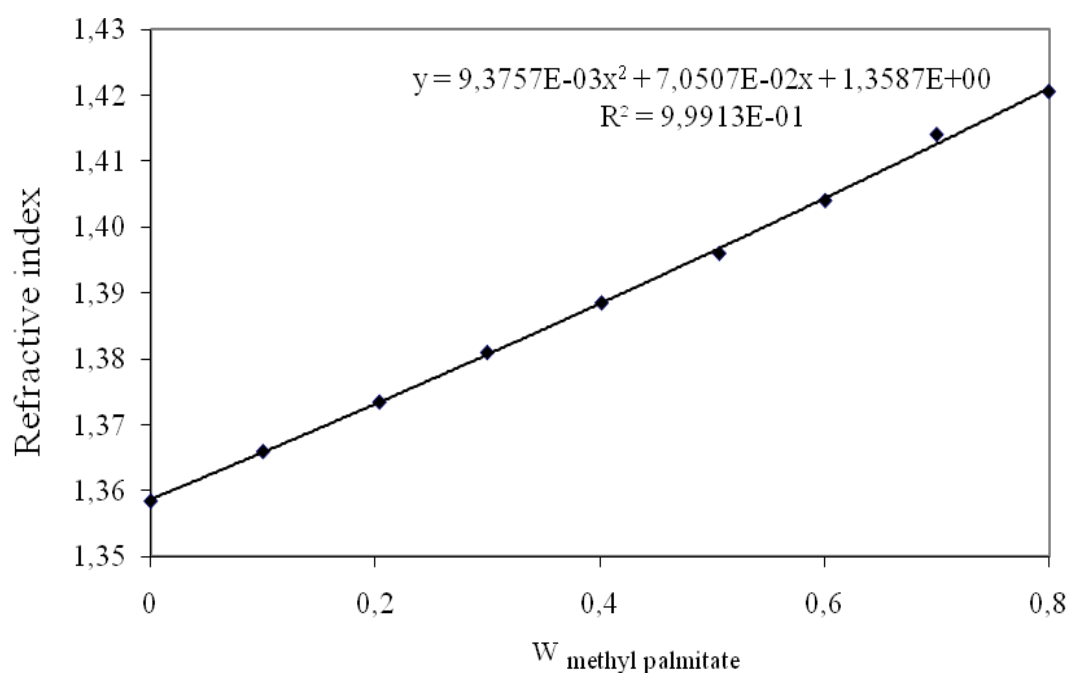


Figure A 3 Calibration curve of ethanol + methyl palmitate system.

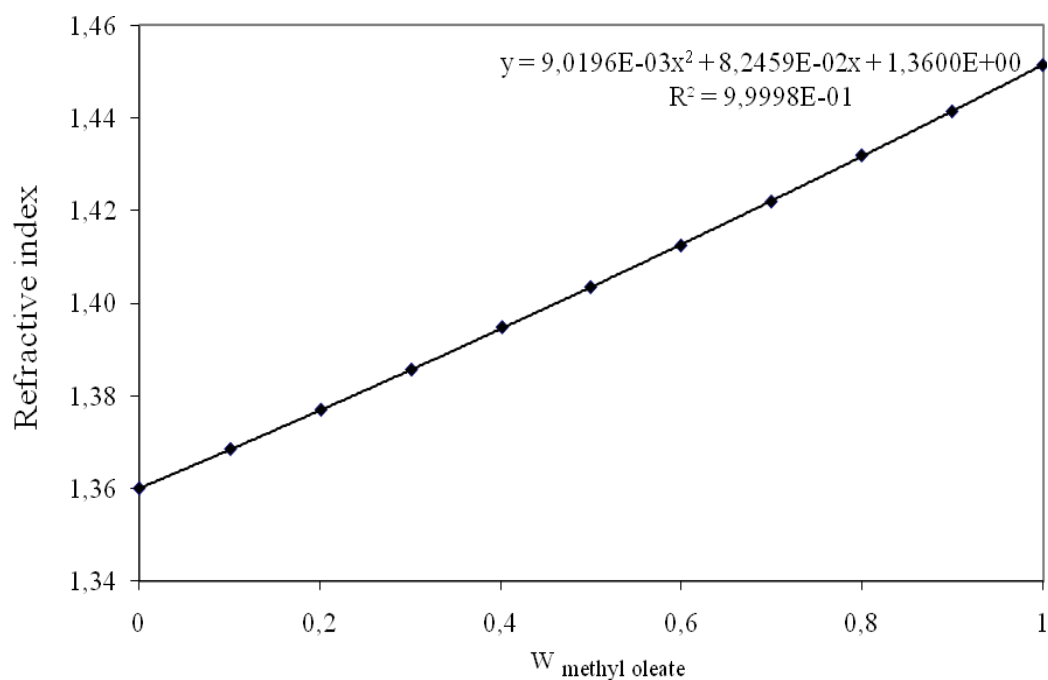
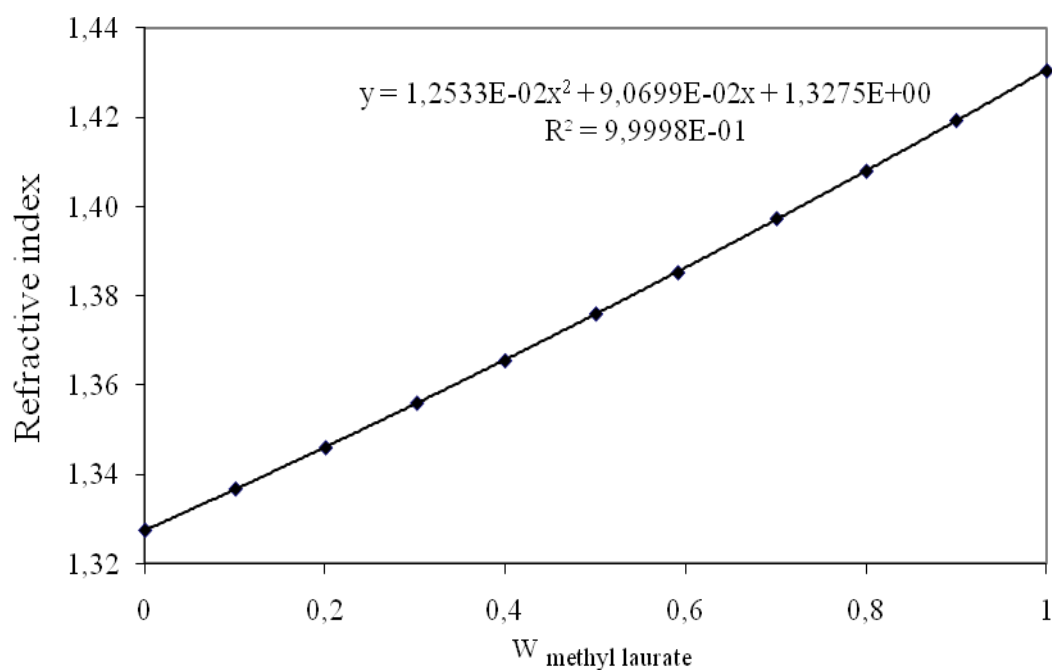
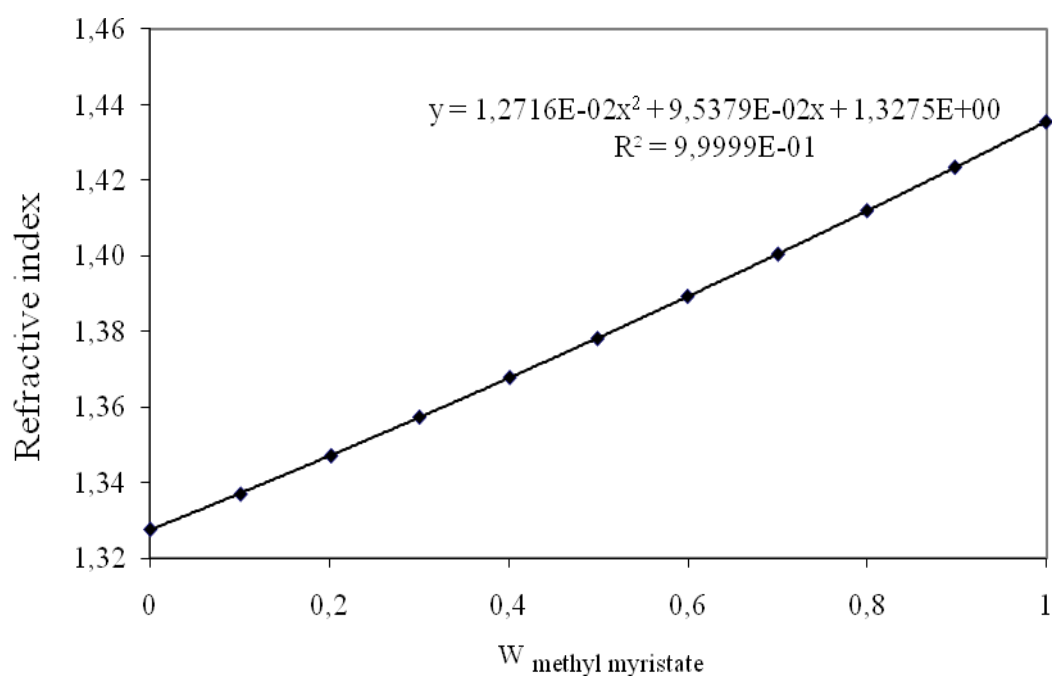


Figure A 4 Calibration curve of ethanol + methyl oleate system.

B. Calibration curves for methanol + FAME systems**Figure B 1** Calibration curve of methanol + methyl laurate system.**Figure B 2** Calibration curve of methanol + methyl myristate system.

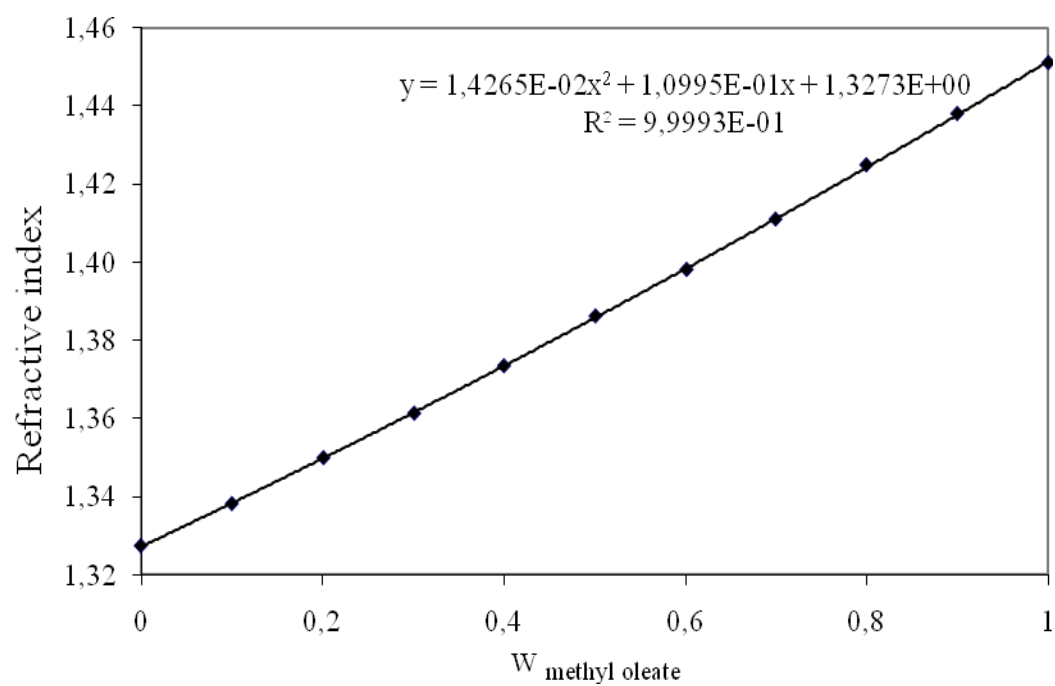


Figure B 3 Calibration curve of methanol + methyl oleate system.